Supplementary data

Secondary metabolites of the leaves of *Tricalysia atherura* N. Hallé (Rubiaceae) and their potential antiplasmodial activity

Gwladys Djikam Sime[a,e], Mbabi Nyemeck II Norbert[a,c], Auguste Abouem A Zintchem[a,b], Natasha October[d], Marius Balemaken Missi[a,d], Rabia Farooq[e], Khalid Mohammed Khan[e], Dominique Serge Ngono Bikobo[a]*, Muhammad Iqbal Choudhary[e], Dieudonné Emmanuel Pegnyemb[a]

[a] *Faculty of science, Department of Organic Chemistry, University of Yaoundé 1, Yaoundé, Cameroon ;*

[b] *Department of Chemistry, Higher Teacher's Training College, University of Yaoundé 1, P.O. Box 47, Yaoundé, Cameroon*;

[c] *Department of Chemistry, Faculty of Science, University of Dschang, P.O. Box 67, Dschang, Cameroon;*

[d] *Department of Chemistry, University of Pretoria, Hatfield 0028, South Africa;*

[e] *International Center for Chemical and Biological Sciences, H.E.J Research Institute of Chemistry, University of Karachi, Karachi-75270, Pakistan;*

ABSTRACT:

One monoterpene indole alkaloid, atheruramine (**1**) bearing an ether bridge linking, one hydrobenzoin derivative, tricalydioloside (**2**) and two ursane-type triterpenes, atherurosides (A and B) (**3** and **4**) were isolated from the leaves of *Tricalysia atherura*, together with eight known compounds. The structures of these new compounds were elucidated on the basis of the results of spectroscopic analysis, and the relative configurations of compounds **1**−**3** were established by NOE difference. Four of the metabolites were screened *in vitro* against both chloroquine (CQ)-sensitive (3D7) and -resistant (Dd2) strains of *Plasmodium falciparum*; they were found to exhibit moderate activity against chloroquine-resistant (Dd2) (IC_{50} 64.99–92.29 μg/mL). Meanwhile, crude extract possesses high antiplasmodial activity against both 3D7 and Dd2 strains of *P. falciparum* (IC_{50} 4.39–7.54 μg/mL) and high selectivity indices values (SI > 10) and was found to be safe.

Keywords: *Tricalysia atherura*, Rubiaceae, indole alkaloid, atheruramine, hydrobenzoin derivative, pentacyclic triterpenes, antiplasmodial and cytotoxic activities.

Experimental

General experiment procedure

Optical rotations were measured with a P2000 automatic digital Polarimeter. UV spectra were recorded on a Hitachi U-3200. IR spectra were recorded on a shimadzu 8900 FT- IR spectrophotometer in KBr disks. NMR spectra were recorded on Bruker Avance- 400, Avance- 500, Avance- 600 MHz using TMS as an internal standard, with chemical shifts recorded as δ values. ESI-MS data were obtained on an ion-trap (Amazon speed) spectrometer (Bruker, Germany). HRESI-MS were performed on a MicrOTOF-Q mass spectrometer (Bruker). The EI-MS and HREI-MS were measured on a Jeol JMS-600H mass spectrometer. Preparative HPLC was carried out on a Japan Analytical Instrument with a LC- 908 W detector using a sil-d-60-80A. Column (250 × 20 mm, 4μm) for a normal phase and ODS H-80 column for reverse phase. Analytical thin layer chromatography (TLC) was performed on precoated silica gel plates (Merck 60 PF_{254}; 20 × 20; 0.25 mm). Circular dichroism was performed on a JASCO J-810 CD spectrophotometer. Column chromatography (CC) was carried out on silica gel (70-230 Mesh; Merck), Sephadex LH-20 (40–70 μm, Amersham Biosciences, Sweden), and vacuum liquid chromatography (VLC) was performed using silica gel 60 (0.04–0.063 mm; 500 g; Merck, Darmstadt, Germany).

LC-MS general procedure

High resolution mass spectra (HRESI-MS) were obtained with a QTOF Spectrometer (Bruker, Germany) equipped with a HESI source. The spectrometer was operated in positive mode (mass range: 100-1500, with a scan rate of 1.00 Hz) with automatic gain control to provide high-accuracy mass measurements within 2 ppm deviation using Na Formate as calibrant. The following parameters were used for experiments: spray voltage of 4.5 kV, capillary temperature of 200 °C. Nitrogen was used as sheath gas (10 l/min). The spectrometer was attached to an Ultimate 3000 (Thermo Fisher, USA) HPLC system consisting of LC-pump, Diode Array Detector (DAD) (λ: 215, 254, 280, 330 nm), auto sampler (injection volume 5 μl) and column oven (50 °C). The separations were performed using a Synergi MAX-RP 100A (50 x 2 mm, 2.5μ particle size) with a H_2O (+0.1 % HCOOH) (A)/acetonitrile (+0.1 % HCOOH) (B) gradient (flow rate 500 μL/min). Samples were analyzed using a gradient program as follows: 95 % A isocratic for 1.5 min, linear gradient to 100 % B over 6 min, after 100 % B isocratic for 2 min, the system returned to its initial condition (90 % A) within 1 min, and was equilibrated for 1 min.

Plant material

The leaves of *Tricalysia atherura* were collected in March 2019 from Mont Kala, in the Center region of Cameroon. Authentication and identification of plant was carried out by Mr. Victor Nana (Botanist). A voucher specimen (N^o 23507/ HNC) was deposited at the National Herbarium in Yaounde, Cameroon.

Extraction and isolation

The dried leaves of *T. atherura* (500 g) were powdered and extracted with MeOH (3 × 2 L) at room temperature for a week. After solvent was removed under reduced pressure, the residue (60 g) was suspended in water and then partitioned with *n*-hexane, CH_2Cl_2, EtOAc and *n*-BuOH respectively. The EtOAc-soluble fraction (3.86 g) was chromatographed on a silica gel column (7 × 50 cm) using a stepwise gradient of *n*-Hex/ EtOAc (100/0 to 0/100, *v/v*), followed by EtOAc/ MeOH (100/0 to 0/100, *v/v*) to give six sub-fractions (TA1 – TA6). Fraction TA3 (0.41 g) was chromatographed on a silica gel column (4 × 45 cm) eluted with a step gradient of *n*-Hex/ EtOAc (80/20 to 100/0, *v/v*) to give three sub-fractions (TA3a – TA3c). Sub-fraction TA3a (23 mg) was chromatographed using Sephadex LH-20 (MeOH 100%) to afford compound **7** (17 mg). Sub-fraction TA3c (17 mg) was also purified using Sephadex LH-20 gel CC, eluted with pure MeOH to yield compound **5** (5.4 mg). Fraction TA4 (0.75 g) was was subjected to silica gel column (4 × 45 cm) eluted with a step gradient of *n*-Hex/AcOEt (100/0 to 0/100, *v/v*) to give two fractions (TA4a and TA4b). Fraction TA4b (0.41 mg) was resubjected to silica gel chromatography (4 × 45 cm), and was purified by preparative TLC using *n*-Hex/ EtOAc (70/30 v/v) to yield **10** (15.0 mg) and **11** (7.0 mg). Fraction TA5 (452 mg) was further separated on a silica gel column (5 × 45 cm) and eluted with CH_2Cl_2-MeOH gradient (30/1 to 5/1, *v/v*) to give four sub-fractions (TA5a-TA5d). Further silica gel chromatography purification of TA5a (100 mg) was accomplished by elution with CH_2Cl_2-MeOH system (15/1 to 8/1, *v/v*) to afford **3** (10.0 mg) and **4** (7.3 mg). Sub-fraction TA5c (71 mg) was subjected to silica gel chromatography (5 × 45 cm), eluted with CH_2Cl_2, and then enriched gradually with MeOH to obtain three fractions (TA5c1-TA5c3). Fraction TA5c3 (39 mg) was applied to a Sephadex LH-20 column, eluted with MeOH to afford compounds **6** (3.7 mg), **8** (8.2 mg) and **12** (6.1 mg). Sub-fraction TA5d (95 mg) was purified using Sephadex LH-20 gel column, eluted with MeOH, then separated by semi-preparative HPLC (sil-d-60-80A, 20 ×250 mm, 40% MeOH at 2.4 mL/ min) to yield **2** (4.0 mg, t_R 21.2 min). Fraction TA2 (101 mg) was fractionated by silica gel column (5 × 45

cm) eluted with *n*-Hex/AcOEt (80/20 to 0/100, *v/v*) to give two sub-fractions (TA2a-TA2b). Fraction TA2b (40 mg) was further chromatographed on a Sephadex LH-20 column using MeOH as mobile phase to produce compounds **1** (10.0 mg) and **9** (5.0 mg).

*Atheruramine (**1**)*

White amorphous powder; $[\alpha_D^{25}]$ -43.7 (*c* 1.0, MeOH); m.p. 241–243°C; UV (MeOH) λ_{max}: 225, 272, 290 nm; IR (KBr) ν_{max}: 3385, 2948, 1678, 1620, 1340, 1248 1115, 1041 cm^{-1}; CD Cotton effects: +1.782 (340 nm), –0.881 (316 nm), +0.844 (292 nm).; ^1H (CD_3OD, 500 MHz) and ^{13}C NMR data (CD_3OD, 125 MHz) see Table S1; ESI-MS (pos.): *m/z* 369.3 $[M+H]^+$; HR-ESI-MS: *m*/*z* 369.1805 (calcd. for $C_{21}H_{25}N_2O_4^+$, 369.1809): HR-EI-MS: *m*/*z* 368.1740.

*Tricalydioloside (**2**)*

White amorphous powder; $[\alpha_D^{25}]$ -39.7 (*c* 1.0, MeOH); m.p. 236–238°C; UV (MeOH) λ_{max} = 226, 251 and 260 nm; IR (KBr) ν_{max}: 3380, 2920, 1562, 1455, 1205, 1032 cm^{-1}; CD Cotton effects: +0.765 (338 nm), –0.874 (324 nm), +0.419 (232 nm); ^1H (CD_3OD, 500 MHz) and ^{13}C NMR data (CD_3OD, 125 MHz) see Table S2; ESI-MS (pos.): *m/z* 571.3 $[M+H]^+$; HR-ESI-MS: *m*/*z* 571.2086 (calcd. for $C_{26}H_{35}O_{14}^+$, 571.2084).

*Atheruroside A (**3**)*

White amorphous powder; $[\alpha_D^{25}]$ +40.6 (*c* 1.0, MeOH); m.p. 241–243°C; UV (MeOH): λ_{max} in nm: 201; IR (KBr): 3448, 2979, 1619, 1205, 1110, 1061, 973 cm^{-1}; CD Cotton effects: +0.837 (344 nm), –1.779 (324 nm), +0.252 (282 nm), –18.364 (220 nm),; ^1H (CD_3OD, 500 MHz) and ^{13}C NMR data (CD_3OD, 125 MHz) see Table S3; ESI-MS (pos.): *m/z* 575.6 $[M+H]^+$; HR-ESI-MS: *m*/*z* 575.4068 (calcd. for $C_{35}H_{59}O_6^+$, 575.4075).

*Atheruroside B (**4**)*

White amorphous powder; $[\alpha_D^{25}]$ +42.3 (*c* 1.0, MeOH); m.p. 239–241°C; UV (MeOH): λ_{max} in nm: 201; IR (KBr): 3452, 2968, 1613, 1201, 1105, 1055, 973 cm^{-1}; ^1H (CD_3OD, 500 MHz) and ^{13}C NMR data (CD_3OD, 125 MHz) see Table S3; ESI-MS (pos.): *m/z* 575.6 $[M+H]^+$; HR-ESI-MS: *m*/*z* 575.4066 (calcd. for $C_{35}H_{59}O_6^+$, 575.4075).

Acid hydrolysis of **3** *and* **4**

A solution contained the mixture of two compounds (8 mg) was dissolved in 7% H_2SO_4 (0.5 ml) and refluxed on an aqueous bath at 100°C for 4 hours. The reaction mixture was diluted with H_2O and extracted with CH_2Cl_2. The CH_2Cl_2 layer was evaporated to dryness and purified by preparative TLC over silica gel with CH_2Cl_2-MeOH (9/1) as eluent. An aglycon (3 mg) was isolated and identified as 19*α*-hydroxy-amyrin through direct comparison with authentic samples (**5**) (TLC, MP, and IR). The sugar mixture was dissolved in pyridine and

analyzed by silica gel-TLC with $CHCl_3$/MeOH/H_2O (7:3:0.2). After spraying, apiose gave a clear yellow spot at R_f 0.76, and xylose gave a blue-green spot at *R*f 0.72. The sugar samples were provided by the Department of Biochemistry of the University of Yaounde I.

Assay for antiplasmodial activity

In vitro cultivation of Plasmodium falciparum

Chloroquine-sensitive 3D7 (*Pf*3D7) and resistant Dd2 (*Pf*IDd2) strains of *P. falciparum* were maintained at the Malaria Research Laboratory, International Centre for Genetic Engineering and Biotechnology, New Delhi, India, and used for *in vitro* blood stage testing of antiplasmodial activity of the plant extracts and fractions. *Plasmodium falciparum* culture was maintained according to the method described by Trager and Jensen (1976) with minor modifications (Kaushik et al. 2015), in fresh O positive human erythrocytes suspended at 4% haematocrit in RPMI 1640 16.2 g/L (Sigma-Aldrich, New Delhi, India) containing 25 mM HEPES, 11.11 mM glucose, 0.2% sodium bicarbonate (Sigma-Aldrich, New Delhi, India), 0.5% albumax I (Gibco, Waltham, MA USA), 45 mg/L hypoxanthine (Sigma-Aldrich, New Delhi, India), and 50 mg/L gentamicin (Gibco, Waltham, MA USA) and incubated at 37 °C under a gas mixture of 5% O_2, 5% CO_2 and 90% N_2. Every day infected erythrocytes were transferred into fresh complete medium to propagate the culture. At parasitaemia > 10%, the cultures were diluted into healthy red blood cells to reduce % parasitaemia to 1–2% so as to maintain the cultures in stress free conditions.

In vitro antiplasmodial assay

Crude extract and fractions were evaluated for antiplasmodial activity against *P. falciparum* 3D7 and Dd2 strains. For drug screening, the SYBR green I-based fluorescence assay was set up as described by Smilkstein et al. (2004). Precisely, 100 μL of Sorbitol-synchronized parasites (Lambros and Vanderberg 1979) were incubated under normal culture conditions (37 °C, 5% CO_2, 5% O_2, 90% N_2) at 1% parasitaemia and 2% haematocrit in flat-bottomed, 96-well plates (Corning, USA) in the absence or presence of increasing concentrations of crude extracts or fractions for 48 h. Chloroquine (Sigma-Aldrich, New Delhi, India) was used as positive control, while 0.4% (v/v) DMSO was used as the negative control. Upon incubation, 100 μL of SYBR green I lysis buffer (Tris (20 mM; pH 7.5), EDTA (5 mM), saponin (0.008%, w/v), and Triton X-100 (0.08%, v/v) was added to each well and mixed gently twice, then incubated in dark at 37°C for 1 h. Fluorescence was then measured with a Victor fluorescence multiwell plate reader (Perkin Elmer, Waltham, MA, USA) with excitation and emission wavelength bands centred at 485 and 530 nm, respectively. The

fluorescence counts were plotted against drug concentration and the 50% inhibitory concentration (IC_{50}) was determined by analysis of dose–response curves using non-linear regression.

Cytotoxicity evaluation on Vero cell lines

The evaluation of cytotoxicity by MTT assay on the VERO cells (monkey epithelial cell line, Sigma-Aldrich) was done according to Mosmann (1983) with slight modifications. Briefly, cells (5.10^4 cells/mL) in 100 µL of complete medium, [MEM with 10% foetal calf serum (FCS), 2 mM L-glutamine and antibiotics (100 µg/mL penicillin and 100 µg/mL streptomycin), NEAA 1X for VERO cell line] were seeded into each well of 96-well plates and incubated at 37°C, 5% CO_2. After 24 h incubation, 100 µL of medium with various product concentrations and appropriate controls (DMSO and doxorubicin) were added and the plates were incubated for 72 h at 37°C, 5% CO_2. Each plate well was then microscope-examined to detect possible precipitate formation before the medium was pipetted out of the wells. One hundred µL of MTT solution (0.5 mg/mL in RPMI 1640) was then added to each well and the cells incubated 2 h at 37°C. After this time, the MTT solution was removed and DMSO (100 µL/well) was added to dissolve the resulting formazan crystals. Plates were shaken vigorously for 5 min. Absorbance was measured at 570 nm with a microplate spectrophotometer (EON). Inhibitory concentration 50% (IC_{50}) was defined as the concentration of drug inducing 50% death of VERO cells compared to the control. To classify the cytotoxicity of the extract, the Malaria Group of the University of Yaounde I established a consensus for the samples evaluated: highly toxic < 10 µg/mL, cytotoxic 10–40 µg / mL, moderately cytotoxic 41–100 µg / mL and no cytotoxic > 100 µg / mL.

Table S1. ^1H and ^{13}C NMR spectroscopic data for compound **1** (500 MHz for ^1H and 125 MHz for ^{13}C, CD_3OD).

Position	atheruramine (**1**)	
	δ_H (*J* in Hz)	δ_C
2	-	137.6 s
3	4.04 (1H, dd, *J*=9.0, 4.2 Hz)	49.2 d
5	3.40 (1H, dd, *J*=7.5, 4.0 Hz)	61.2 d
6*α*	3.09 (1H, dd, *J*=16.5, 1.5 Hz)	24.6 t
6*β*	3.00 (1H, dd, *J*=16.0, 5.0 Hz)	
7	-	104.7 s
8	-	127.8 d
9	7.36 (1H, d, *J*=8.0 Hz)	118.4 d
10	6.96 (1H, dd, *J*=8.0, 7.8 Hz)	119.7 d
11	7.04 (1H, dd, *J*=8.0, 7.6 Hz)	122.1 d
12	7.27 (1H, d, *J*=8.5 Hz)	111.9 d
13	-	138.3 s

14*α*	2.14 (1H, dq, *J*=18.5, 7.0, 5.0, 2.0 Hz)	23.1 t
14*β*	1.95 (1H, m)	
15	2.22 (1H, dd, *J*=7.0, 4.0 Hz)	38.6 d
16	-	53.9 s
17	2.88 (2H, brs)	63.2 t
18	3.76 (2H, overlapped)	58.3 t
19*α*	1.98 (1H, m)	38.1 t
19*β*	1.82 (1H, ddd, *J*=14.0, 7.0, 6.8 Hz)	
20	-	84.1 s
21	-	172.8 s
22*α*	3.75 (1H, overlapped)	76.3 t
22*β*	3.67 (1H, d, *J*=14.0 Hz)	
N–Me	3.07 (3H, s)	51.6 s

Table S2. ^{1}H and ^{13}C NMR spectroscopic data for compound **2** (500 MHz for ^{1}H and 125 MHz for ^{13}C, CD_3OD).

Position	tricalydioloside (**2**)	
	δ_H (*J* in Hz)	δ_C
1	5.95 (1H, brs)	68.4 d
2	5.81 (1H, brd, *J*= 1.0 Hz)	68.2 d
1′	-	136.3 s
2′	6.99 (1H, overlapped)	115.7 d
3′	-	189.3 s
4′	6.85 (1H, overlapped)	118.0 d
5′	7.24 (1H, dd, *J*=8.0, 7.5 Hz)	131.0 d
6′	7.02 (1H, overlapped)	119.9 d
1″	-	136.0 s
2″	6.99 (1H, overlapped)	115.5 d
3″	-	159.3 s
4″	6.83 (1H, overlapped)	117.6 d
5″	7.25 (1H, dd, *J*=8.0, 7.5 Hz)	131.1 d
6″	7.02 (1H, overlapped)	119.6 d
1‴	4.64 (1H, d, *J*=7.5 Hz)	102.0 d
2‴	3.26 (1H, m)	74.6 d
3‴	3.39 (1H, m)	78.0 d
4‴	3.25 (1H, m)	71.4 d
5‴	3.24 (1H, m)	78.3 d
6‴	3.56 (1H, dd, *J*=11.5, 5.6 Hz)	64.4 t
	3.51 (1H, dd, *J*=11.0, 7.1 Hz)	
1⁗	4.23 (1H, d, *J*=7.5 Hz)	101.8 d
2⁗	3.64 (1H, m)	73.8 d
3⁗	3.23 (1H, m)	78.3 d
4⁗	3.28 (1H, m)	71.4 d
5⁗	3.27 (1H, m)	78.1 d
6⁗	3.91 (1H, dd, *J*=12.0, 2.1 Hz)	62.8 t
	3.67 (1H, m)	

Table S3. ^{1}H and ^{13}C NMR data of compounds **3** and **4** [a] (500 MHz for ^{1}H and 125 MHz for ^{13}C, CD_3OD).

Position	atheruroside A (**3**)		atheruroside B (**4**)	
	δ_H (*J* in Hz)	δ_C	δ_H (*J* in Hz)	δ_C
1	1.76 (1H, m)	38.1 t	1.62 (1H, m)	39.2 t
	1.60 (1H, m)		0.97 (1H, m)	
2	1.81 (1H, m)[a]	26.8 t	1.75 (1H, m)	26.6 t
	1.68 (1H, m)		1.50 (1H, m)	
3	3.12 (1H, m)	90.7 d	3.03 (1H, dd, *J*=9.5, 3.5 Hz)	89.4 d
4	-	40.1 s	-	39.9 s
5	0.78 (1H, m)	57.1 d	0.79 (1H, m)	56.9 d
6	1.52 (1H, m)	19.3 t	1.53 (1H, m)	19.6 t
	n.o		n.o	
7	1.51 (1H, m)	33.6 t	1.55 (1H, m)	34.1 t
			1.31 (1H, m)	
8	-	41.3 s		41.5 s
9	1.67 (1H, m)	48.7 d	1.68 (1H, m)	48.8 d
10	-	39.7 s	-	39.6 s
11	1.93 (1H, m)	24.6 t	1.95 (1H, m)	24.5 t
12	5.27 (1H, m)	129.3 d	5.27 (1H, m)	129.4 d
13	-	140.2 s	-	140.0 s
14	-	42.3 s	-	42.3 s
15	n.o	29.5 t	1.80 (1H, m)	29.4 t
	1.00 (1H, m)[a]		0.97 (1H, m)	
16	1.83 (1H, m)	26.9 t	1.60 (1H, m)	27.2 t
	1.32 (1H, m)			
17	-	42.9 s	-	42.7 s
18	2.51 (1H, m)	55.1 d	2.49 (1H, m)	55.0 d
19	-	73.7 s	-	73.5 s
20	1.33 (1H, m)	42.9 d	1.34 (1H, m)	42.9 d
21	1.31 (1H, m)[a]	28.2 t	1.62 (1H, m)	26.8 t
22	n.o	35.8 t	1.70 (1H, m)	38.9 t
23	1.03 (3H, s)	29.6 q	0.98 (3H, s)	28.3 q
24	0.84 (3H, s)	16.7 q	0.80 (3H, s)	17.1 q
25	0.94 (3H, s)	15.9 q	0.94 (3H, s)	16.1 q
26	0.76 (3H, s)	17.5 q	0.78 (3H, s)	17.3 q
27	1.31 (3H, s)	24.5 q	1.32 (3H, s)	24.6 q
28	0.92 (3H, s)	16.4 q	0.92 (3H, s)	16.4 q
29	1.18 (3H, s)	26.9 q	1.18 (3H, s)	27.0 q
30	0.93 (3H, d, *J* = 6.3 Hz)	16.1 q	0.91 (3H, d, *J* = 6.3 Hz)	16.5 q
1′	4.27 (1H, d, *J*=8.0 Hz)	107.1 d	4.97 (1H, d, *J*=2.5 Hz)	112.5 d
2′	3.56 (1H, m)	72.8 d	3.83 (1H, d, *J*=2.5 Hz)	78.1 d
3′	3.51(1H, m)	74.3 d	-	80.1 s
4′	3.79 (1H, m)	69.3 d	3.98 (1H, d, *J*=8.0 Hz)	74.4 t
			3.71 (1H, d, *J*=8.0 Hz)	
5′ α/*β*	3.81 (1H, m)	66.3 t	3.56 (2H, d, *J*=5.5 Hz)	65.5 t
	3.50 (1H, m)			

[a] Assignments were supported with COSY, HSQC, HMBC and NOESY experiments.
n.o., not observed.

Table S4. The antiplasmodial and cytotoxic activities of the crude extract of the leaves of *T. atherura* and its constituents.

	IC_{50} [a] (µg/ml) (mean ± SD)		CC_{50} (µg/ml) (mean ± SD)	Selectivity index (SI)	
	3D7	**Dd2**	**Vero** [b]	**3D7**	**Dd2**
Leaves extract	7,54± 0,53	4,39±0,27	> 100	> 13.26	> 22.78
1	> 100	64,99±13,65	NP*	NP*	NP*
4	> 100	92,29±3,78	NP*	NP*	NP*
5	> 100	74,88±1,93	NP*	NP*	NP*
8	> 100	73,02±1,02	NP*	NP*	NP*
Artemisinin (µM)	0,034±0,004	0,043±0,011	-	-	-
Chloroquine (µM)	0,0292±0,0003	0,0113±0,0003	-	-	-
Doxorubicin (µM)	-	-	0.62 ± 0.04 µM	-	-

[a] IC_{50}: half maximal inhibitory concentration, given in µM and in µg/mL for crude extract and pure compounds. The mean values of at least three independent experiments are reported;
[b] On Vero cell lines at 72 h of culture.
*NP = not performed.

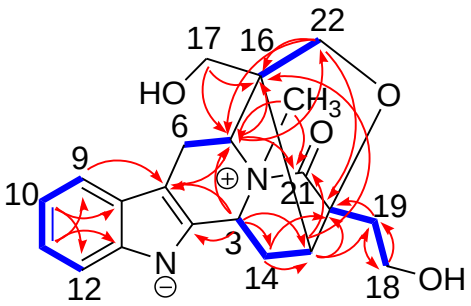

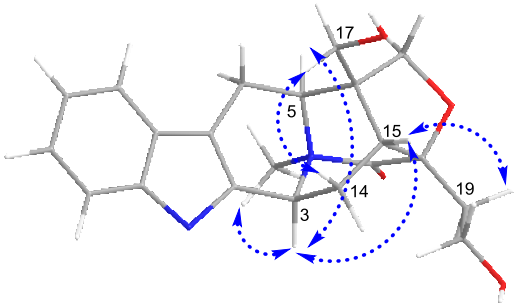

1

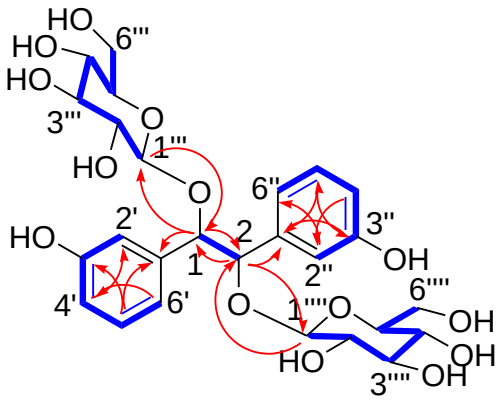

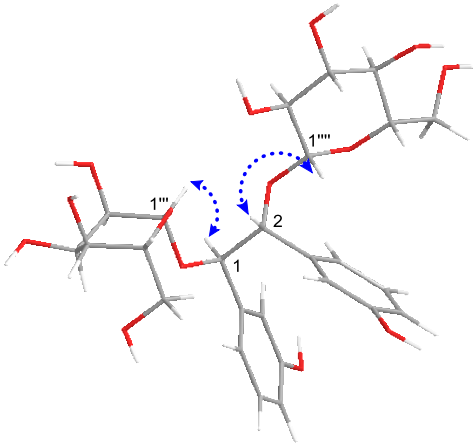

2

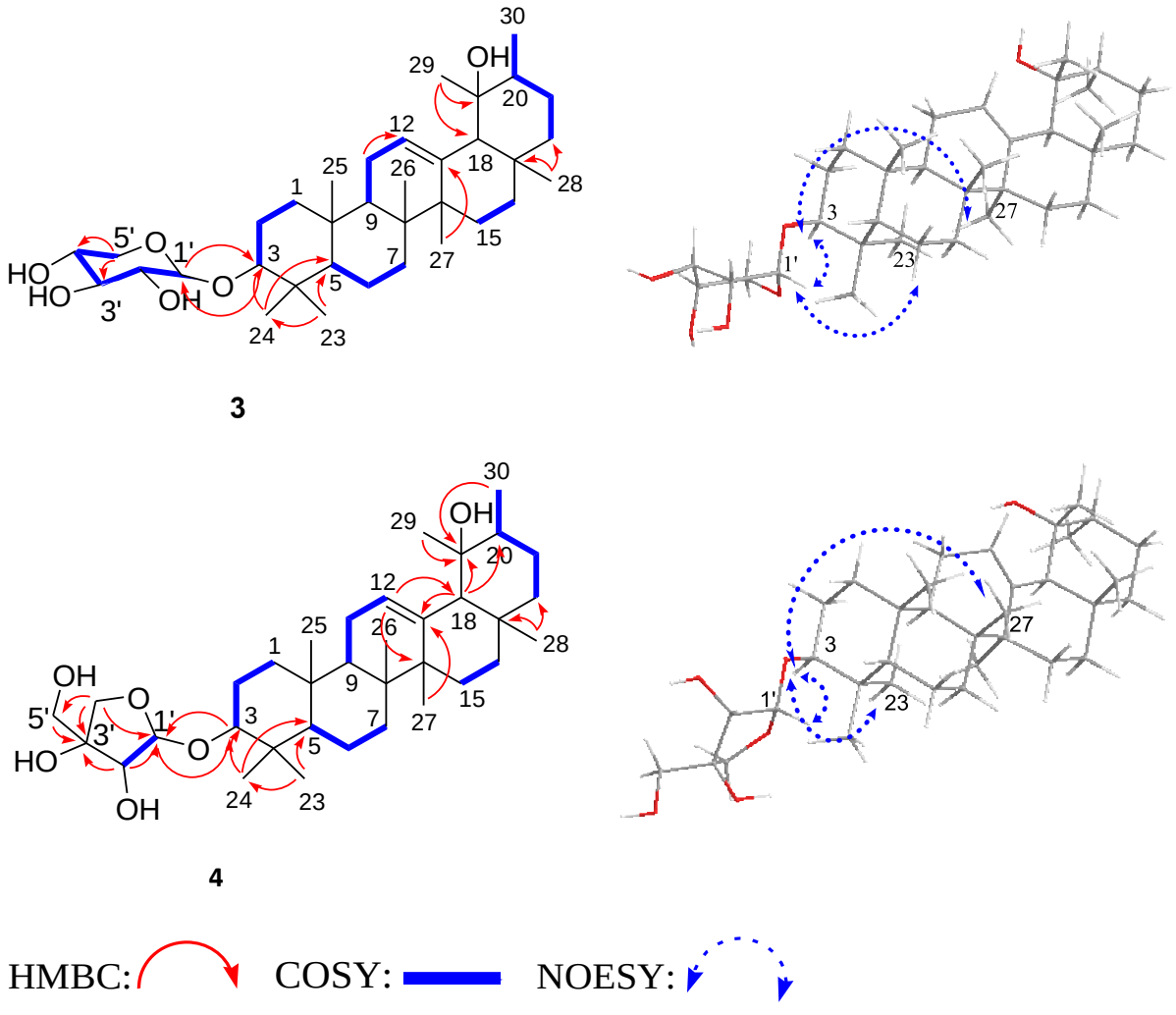

Figure S1 . Selected 2D NMR correlations of **1**–**4.**

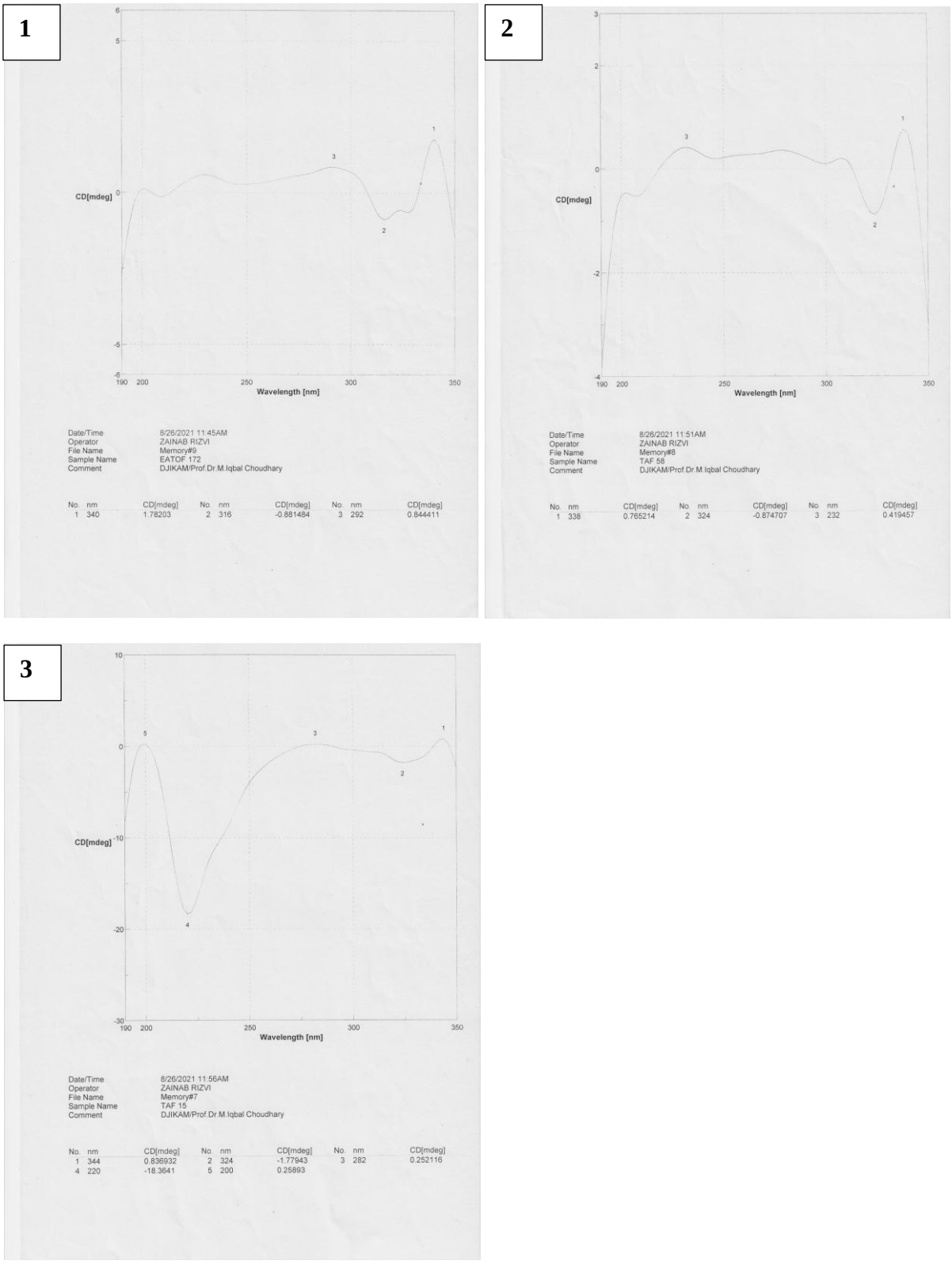

Figure S2. CD spectra for atheruramine, tricalydioloside and atheruroside A (**1, 2** and **3**) (in MeOH).

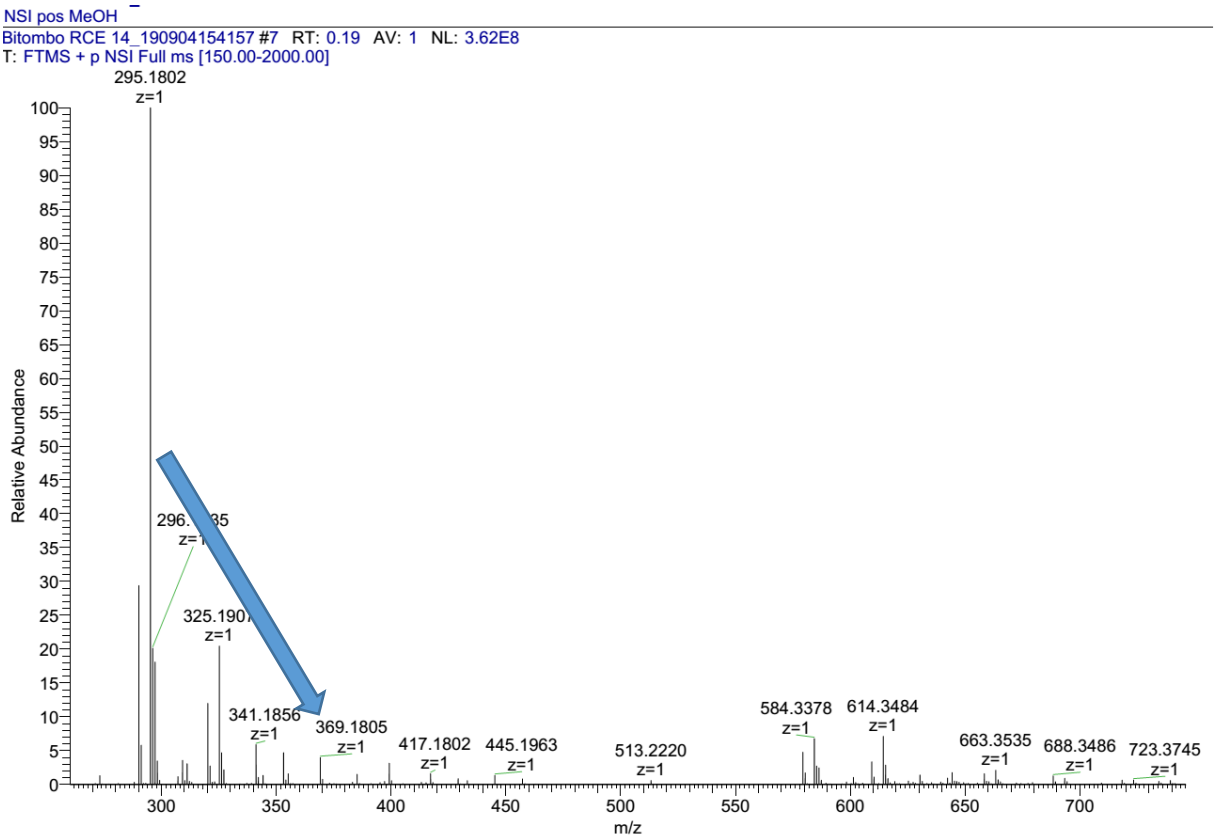

Figure S3 . HR-ESI-MS spectrum of compound **1**.

Mass	Relative Intensity	Theoretical Mass	Delta [ppm]	Delta [mmu]	RDB	Composition
351.1671	1.4	351.1682	-3.0	-1.1	7.0	$C_{18}H_{25}O_6N_1$
		351.1709	-10.7	-3.7	11.5	$C_{21}H_{23}O_3N_2$
		351.1623	13.7	4.8	16.0	$C_{25}H_{21}O_1N_1$
353.1578	2.3	353.1542	10.3	3.6	15.5	$C_{25}H_{21}O_2$
		353.1627	-13.9	-4.9	11.0	$C_{21}H_{23}O_4N_1$
365.1498	1.1	365.1501	-0.9	-0.3	12.5	$C_{21}H_{21}O_4N_2$
		365.1542	-11.9	-4.3	16.5	$C_{26}H_{21}O_2$
366.1576	1.2	366.1580	-0.9	-0.3	12.0	$C_{21}H_{22}O_4N_2$
		366.1620	-11.9	-4.3	16.0	$C_{26}H_{22}O_2$
367.1670	19.8	367.1658	3.4	1.3	11.5	$C_{21}H_{23}O_4N_2$
		367.1698	-7.5	-2.8	15.5	$C_{26}H_{23}O_2$
368.1740	15.1	368.1736	1.0	0.4	11.0	$C_{21}H_{24}O_4N_2$
		368.1776	-9.9	-3.7	15.0	$C_{26}H_{24}O_2$
369.1737	3.4	369.1729	2.4	0.9	15.0	$C_{25}H_{23}O_2N_1$
		369.1702	9.6	3.5	10.5	$C_{22}H_{25}O_5$

Figure S4.HREI-MS spectrum of compound **1.**

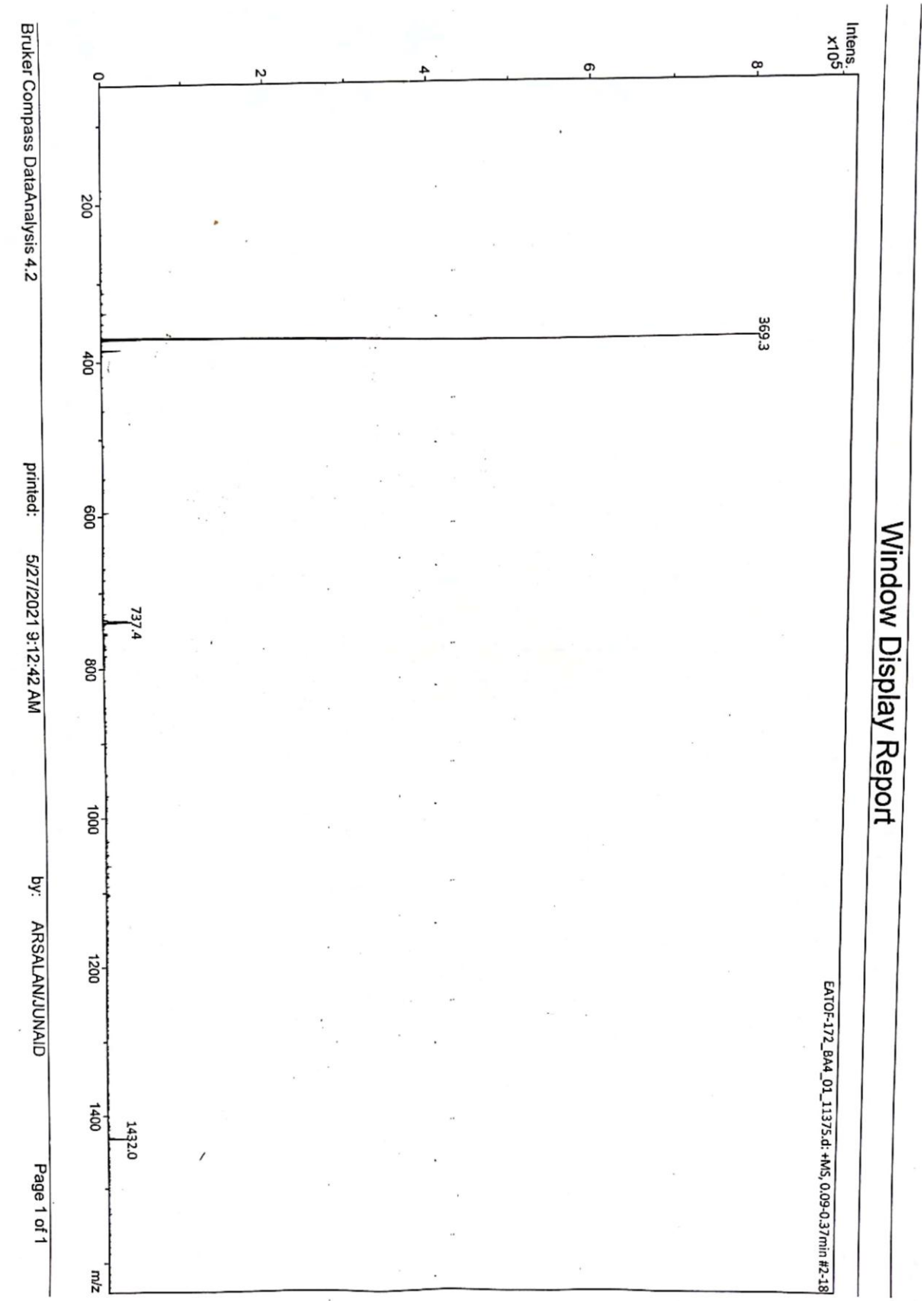

Figure S5. LRESI-MS spectrum of compound **1.**

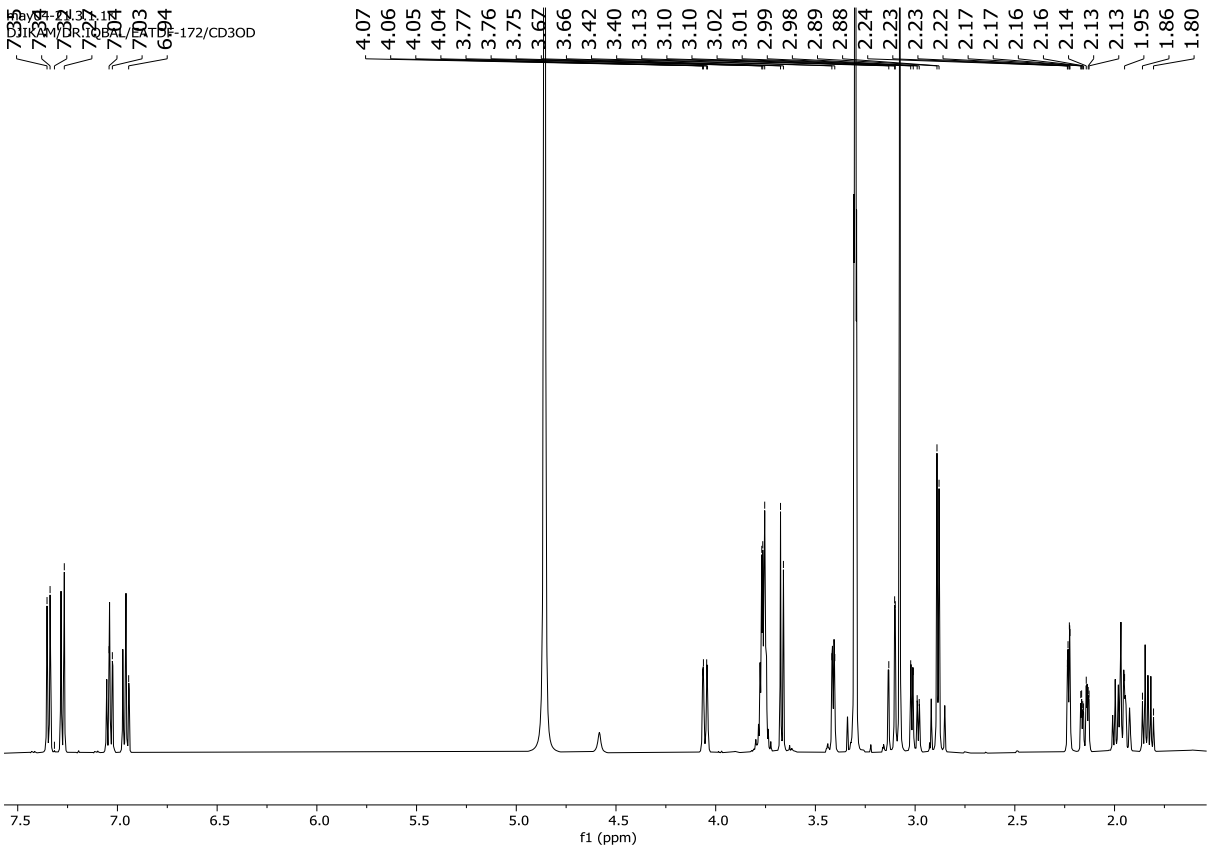

Figure S6. ^{1}H NMR spectrum of compound **1.**

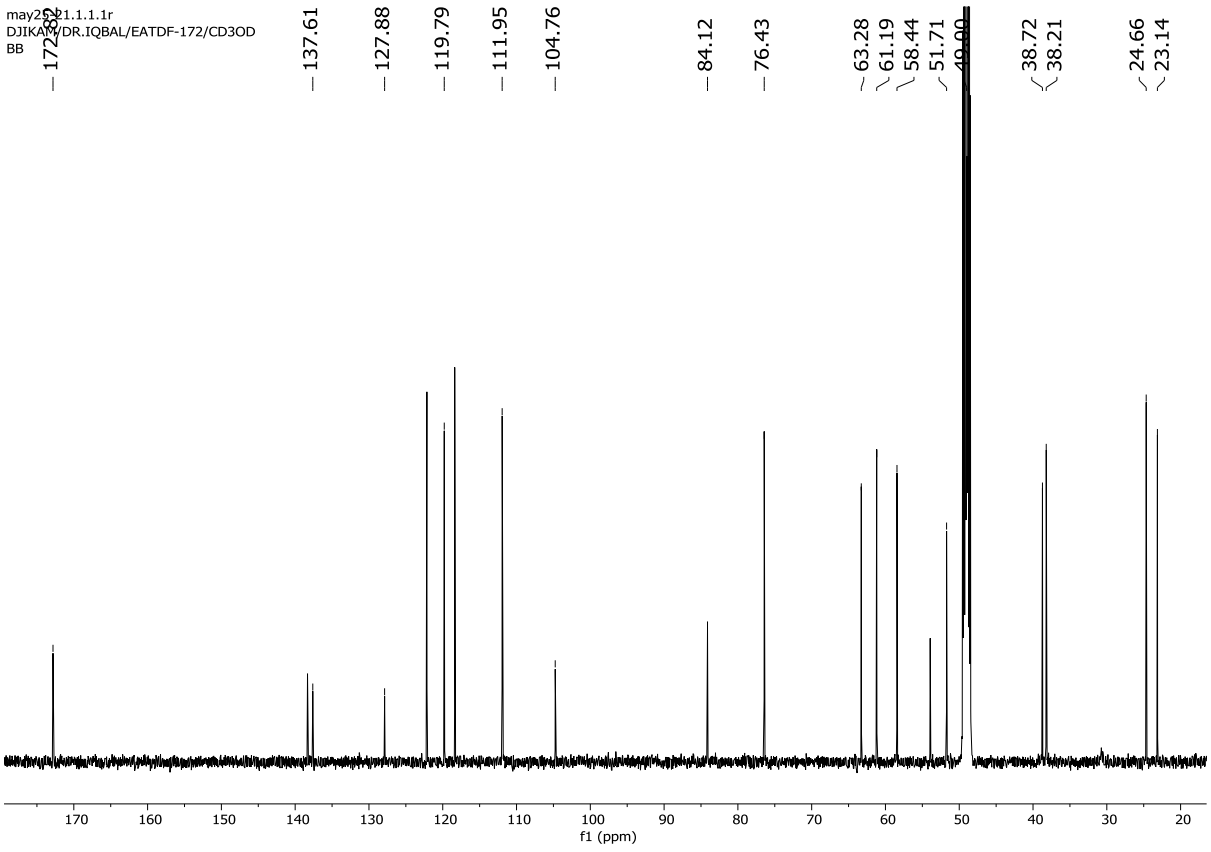

Figure S7. ^{13}C NMR spectrum of compound **1.**

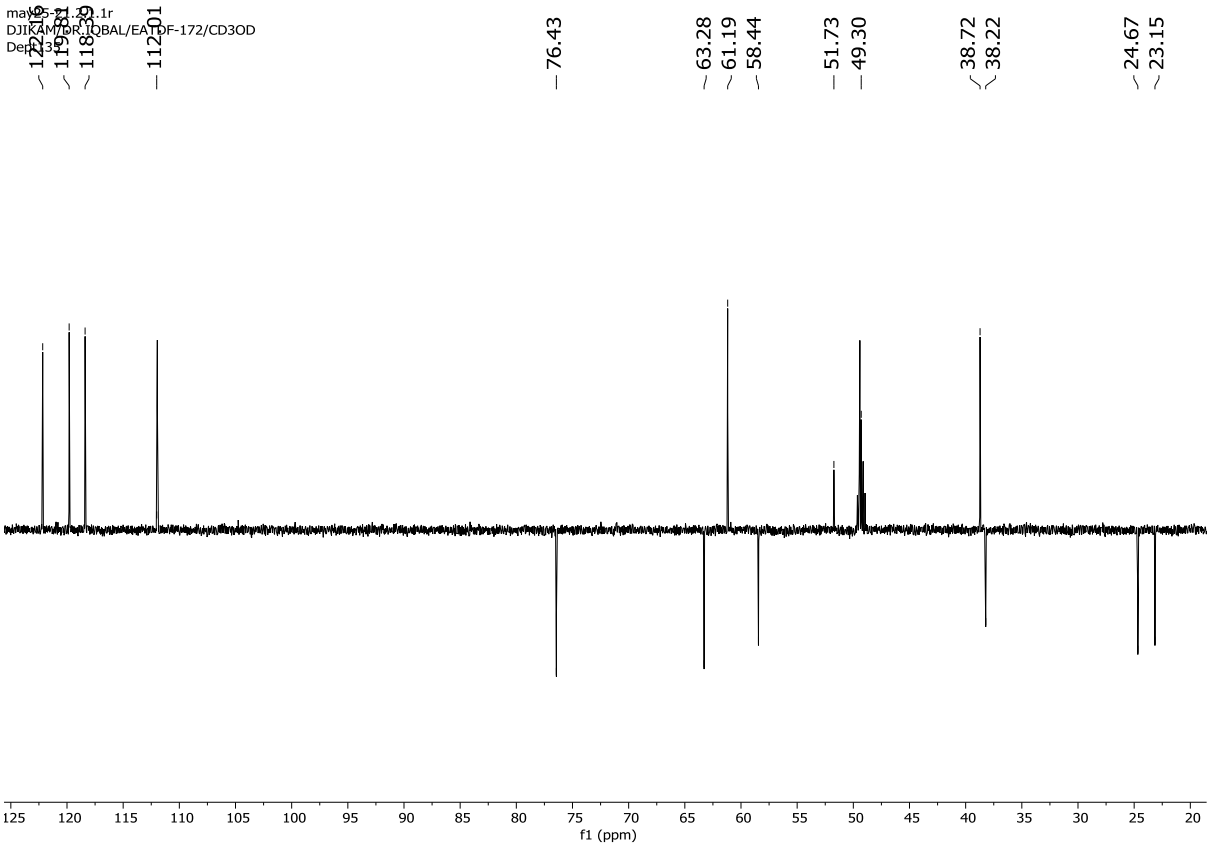

Figure S8. DEPT 135 spectrum of compound **1.**

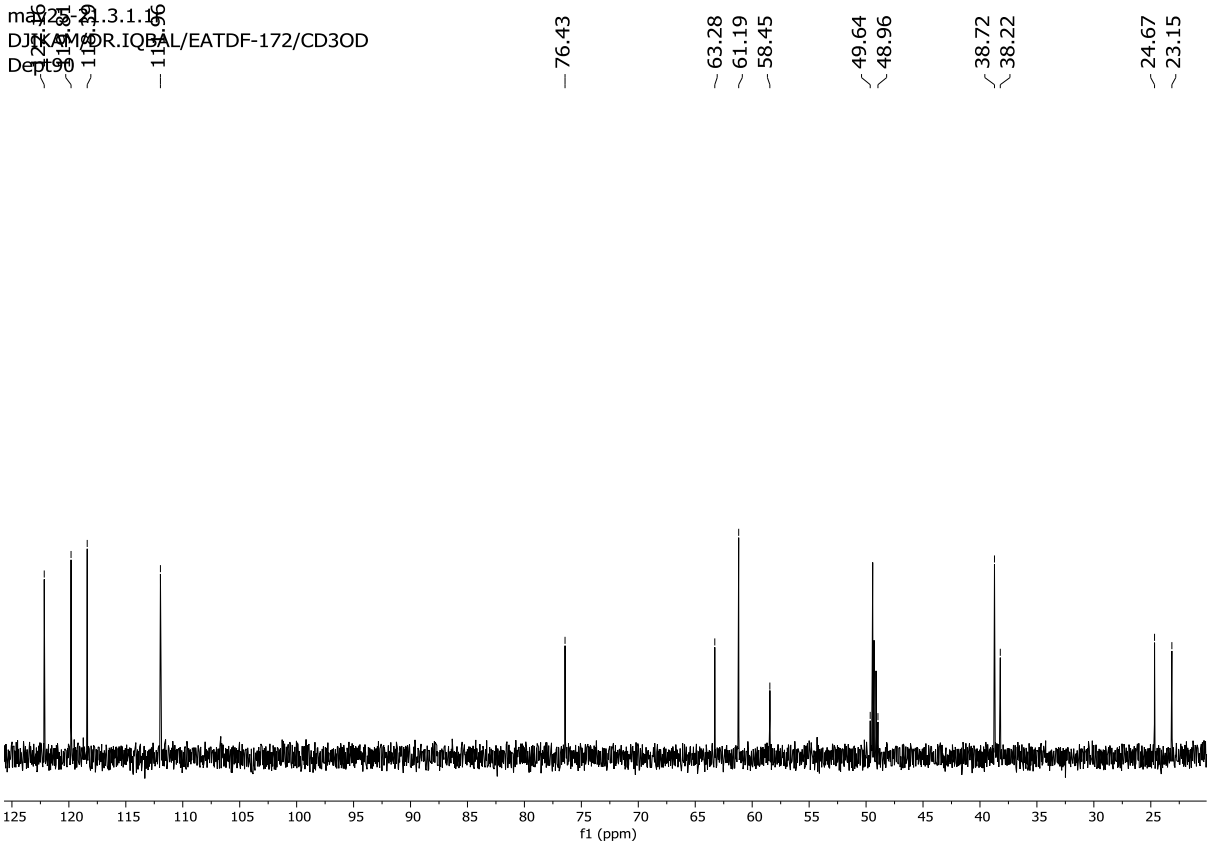

Figure S9. ^{13}C DEPT 90 spectrum of compound **1.**

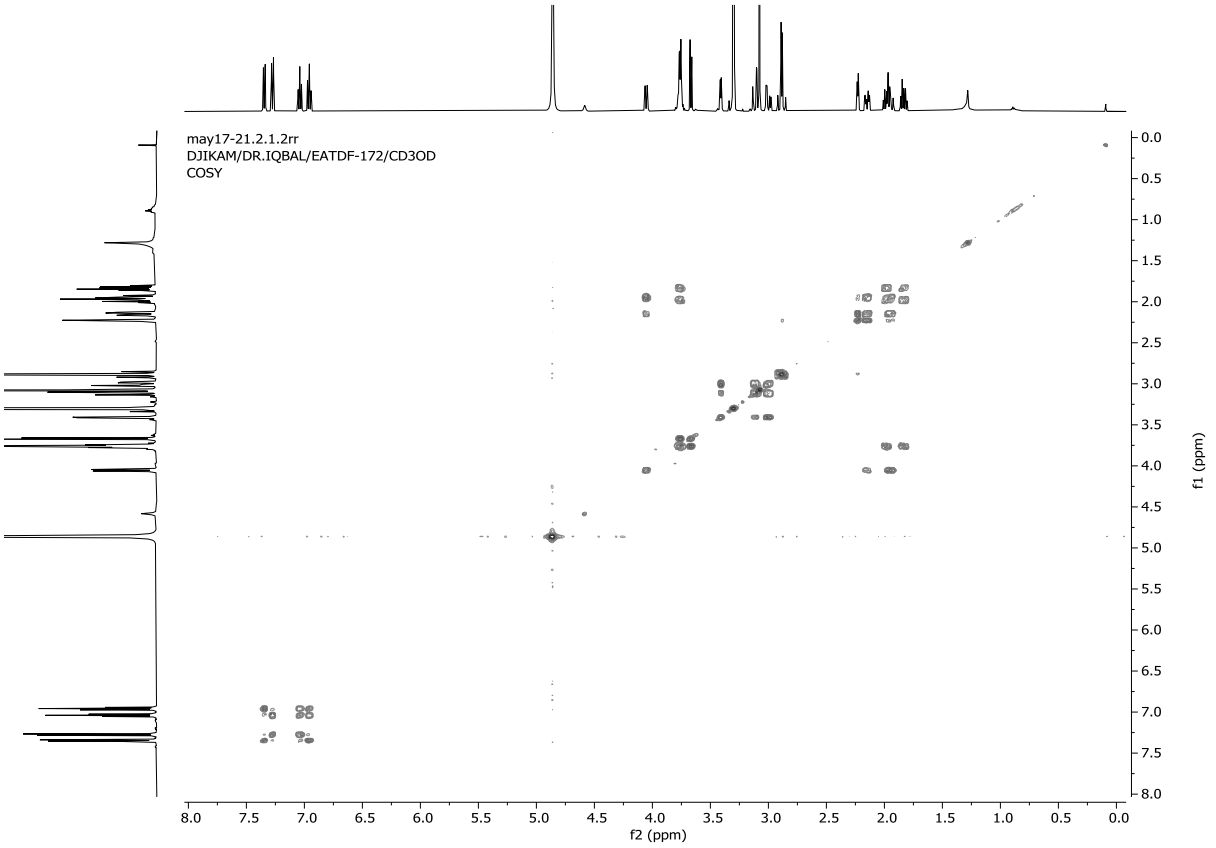

Figure S10. COSY spectrum of compound **1.**

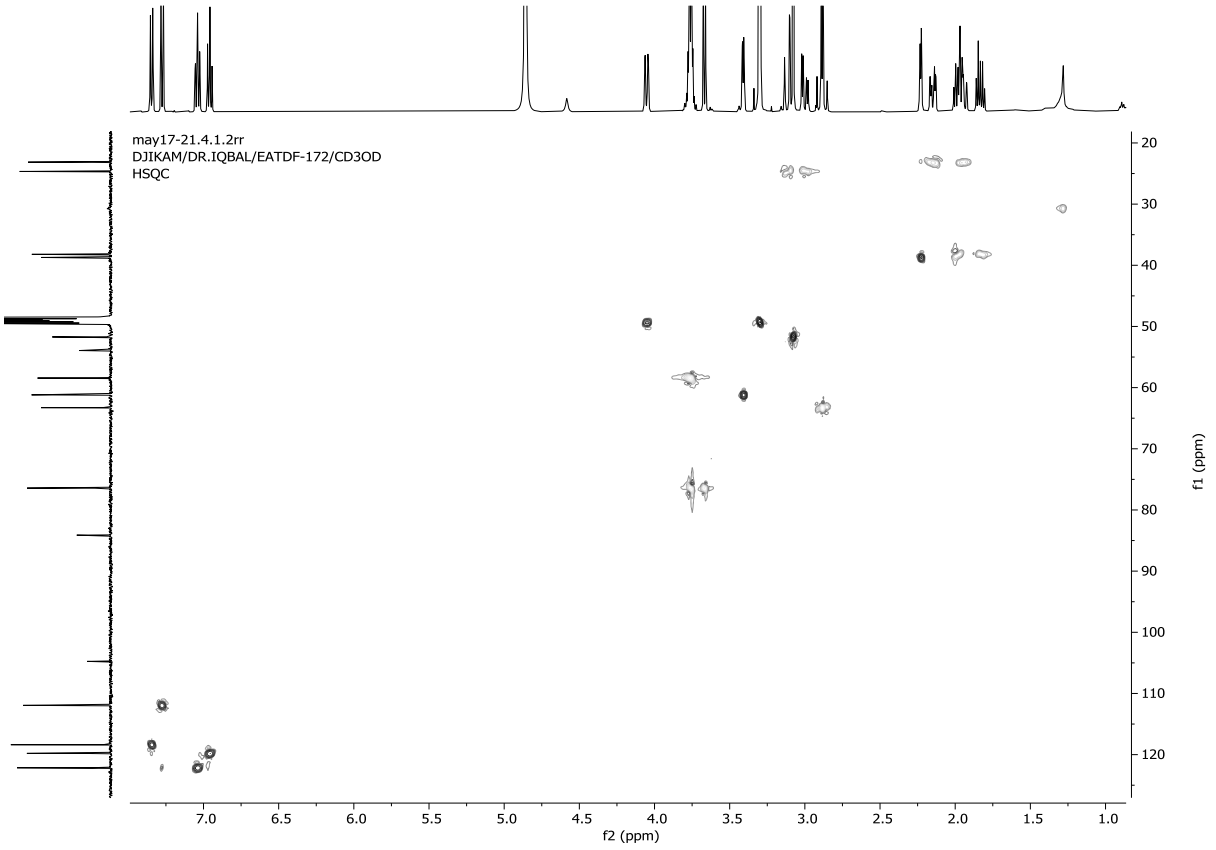

Figure S11. HSQC spectrum of compound **1.**

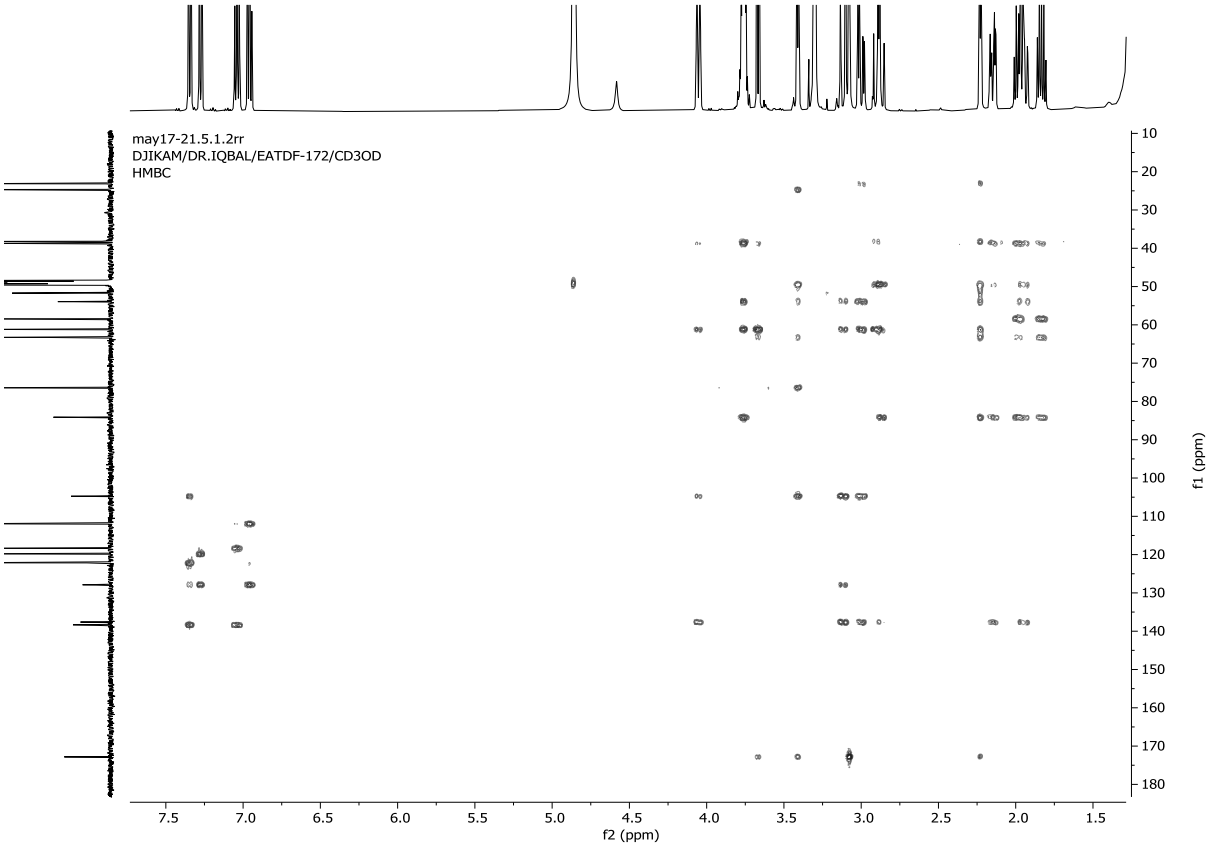

Figure S12. HMBC spectrum of compound **1.**

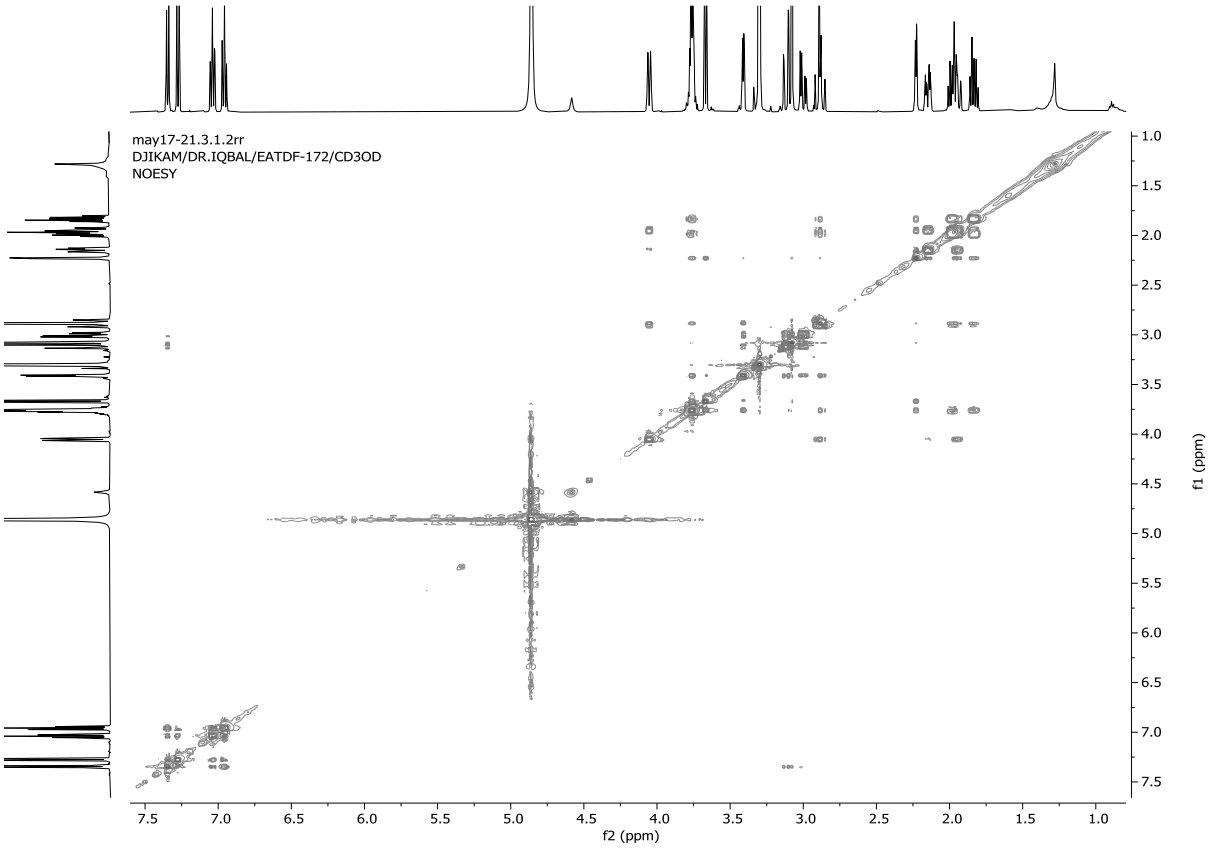

Figure S13. NOESY spectrum of compound **1.**

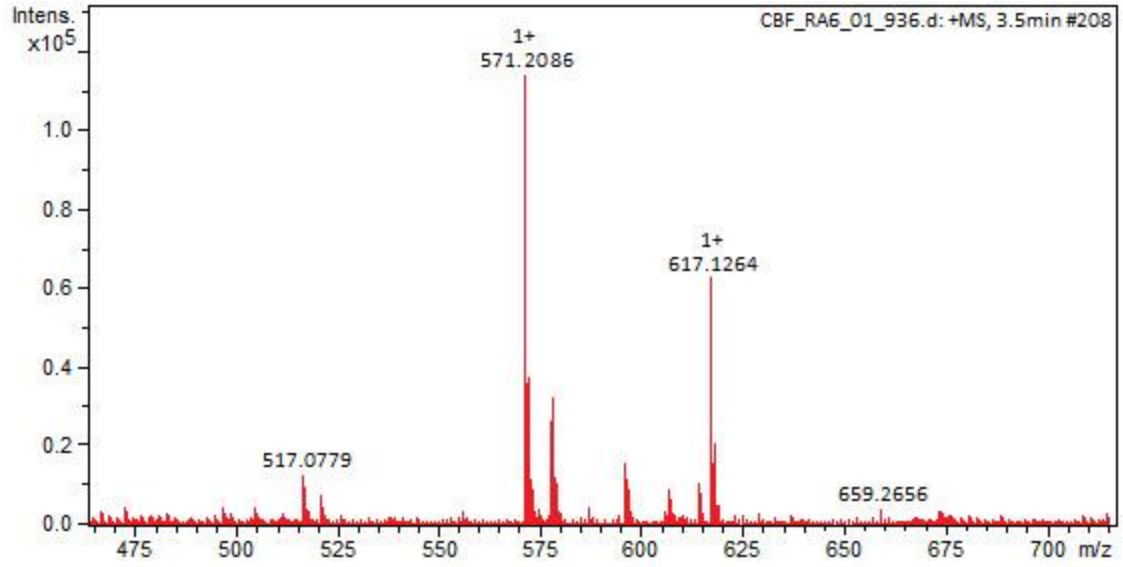

Figure S14 . LC-MS spectrum of compound **2**.

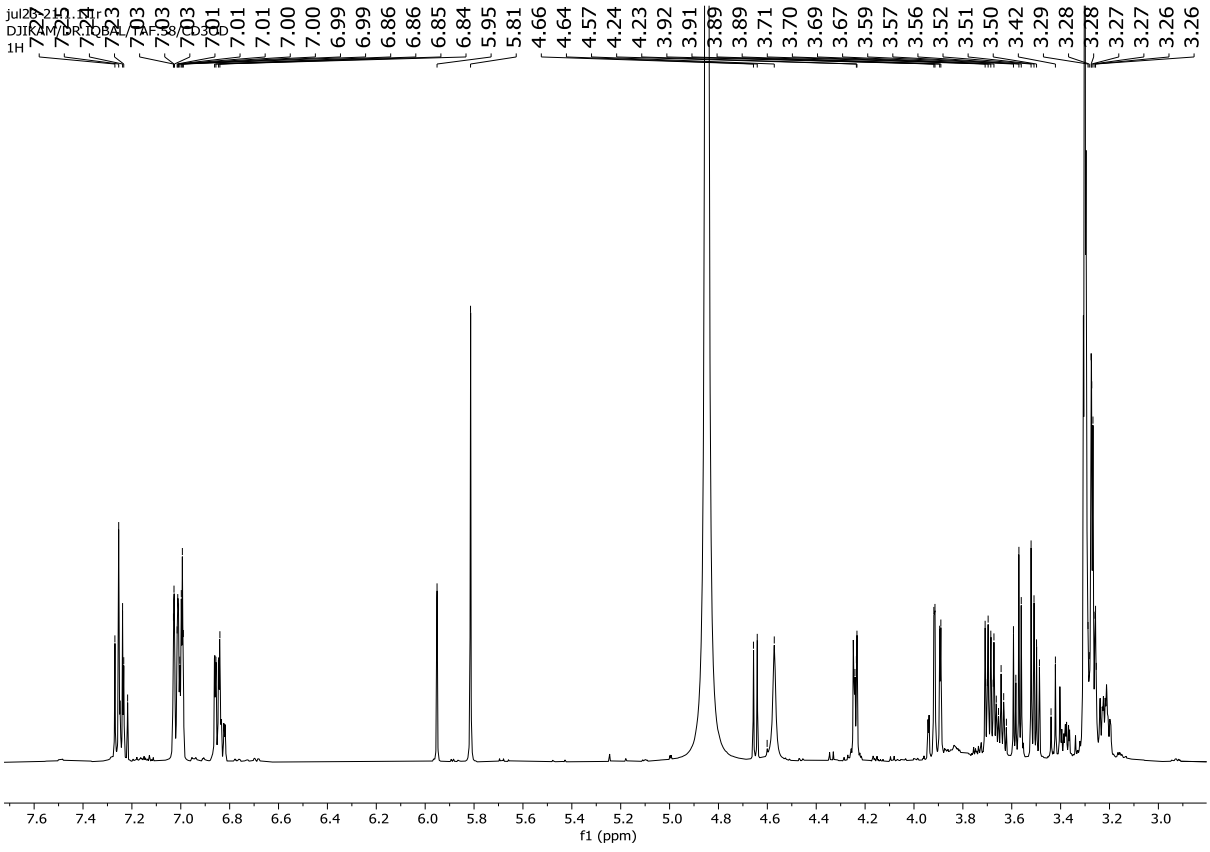

Figure S15. ^{1}H NMR spectrum of compound **2.**

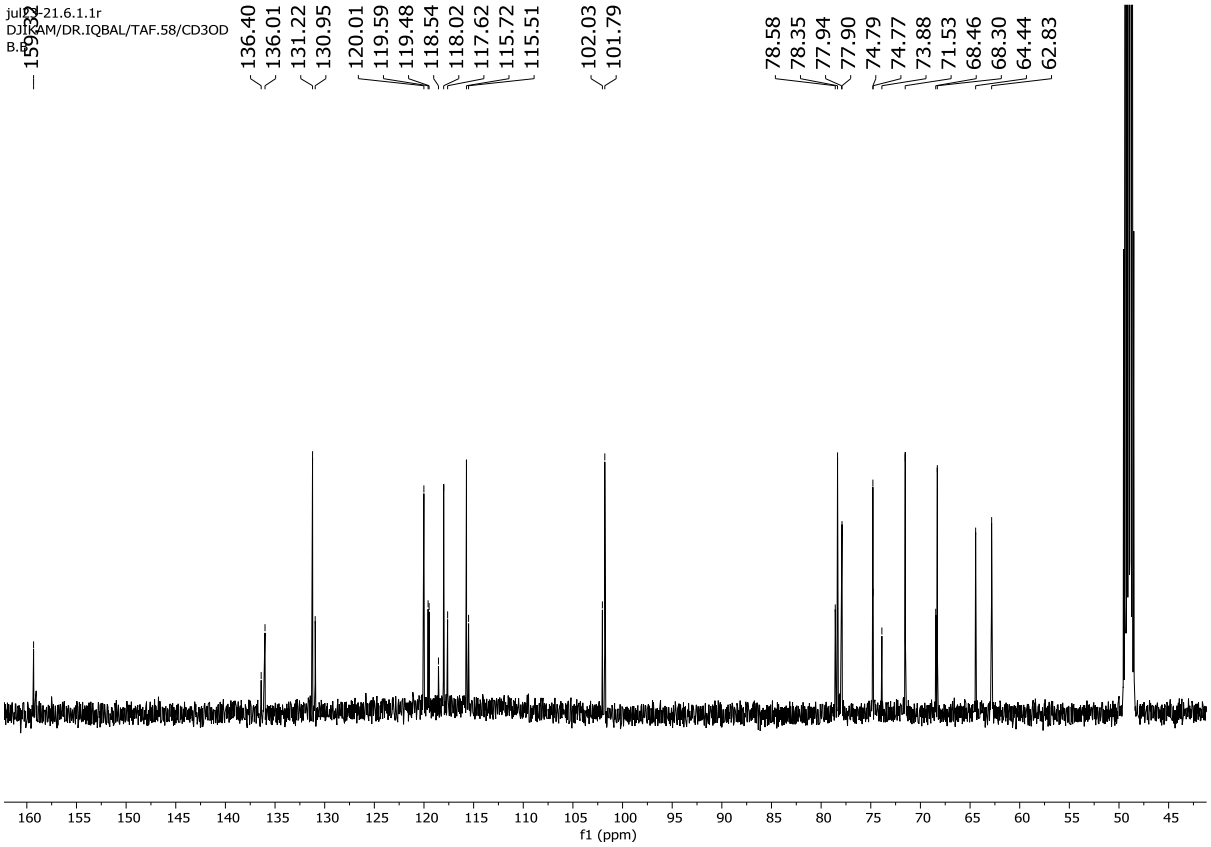

Figure S16. ^{13}C NMR spectrum of compound **2.**

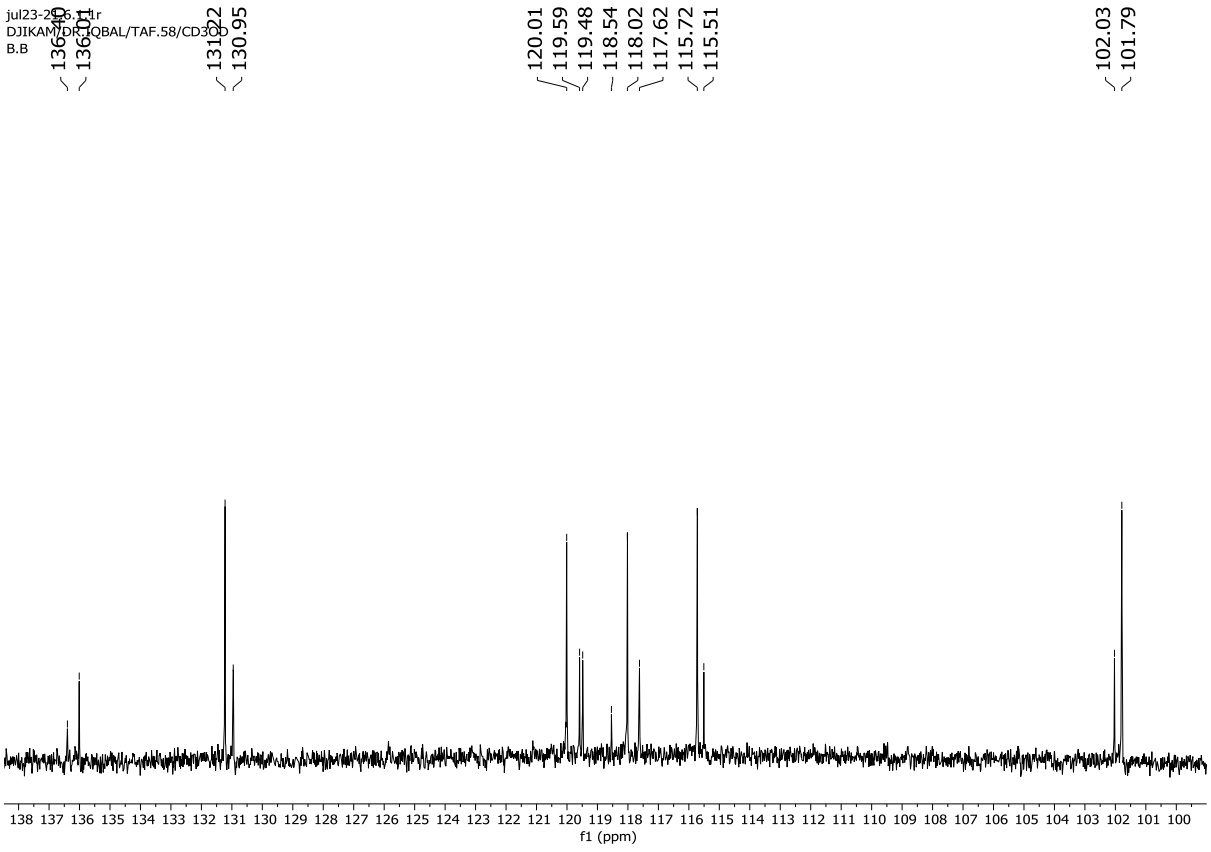

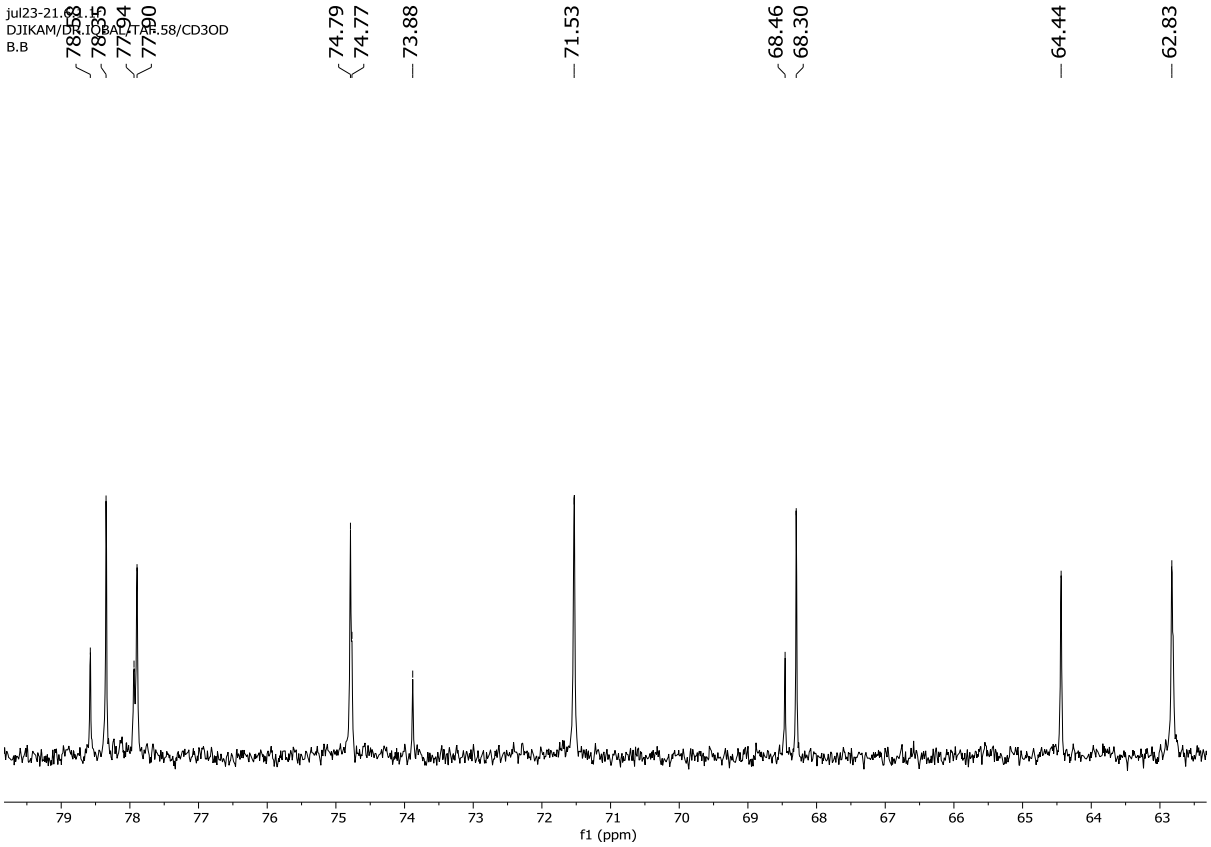

Figure S17. Expanded ^{13}C NMR spectrum of compound **2.**

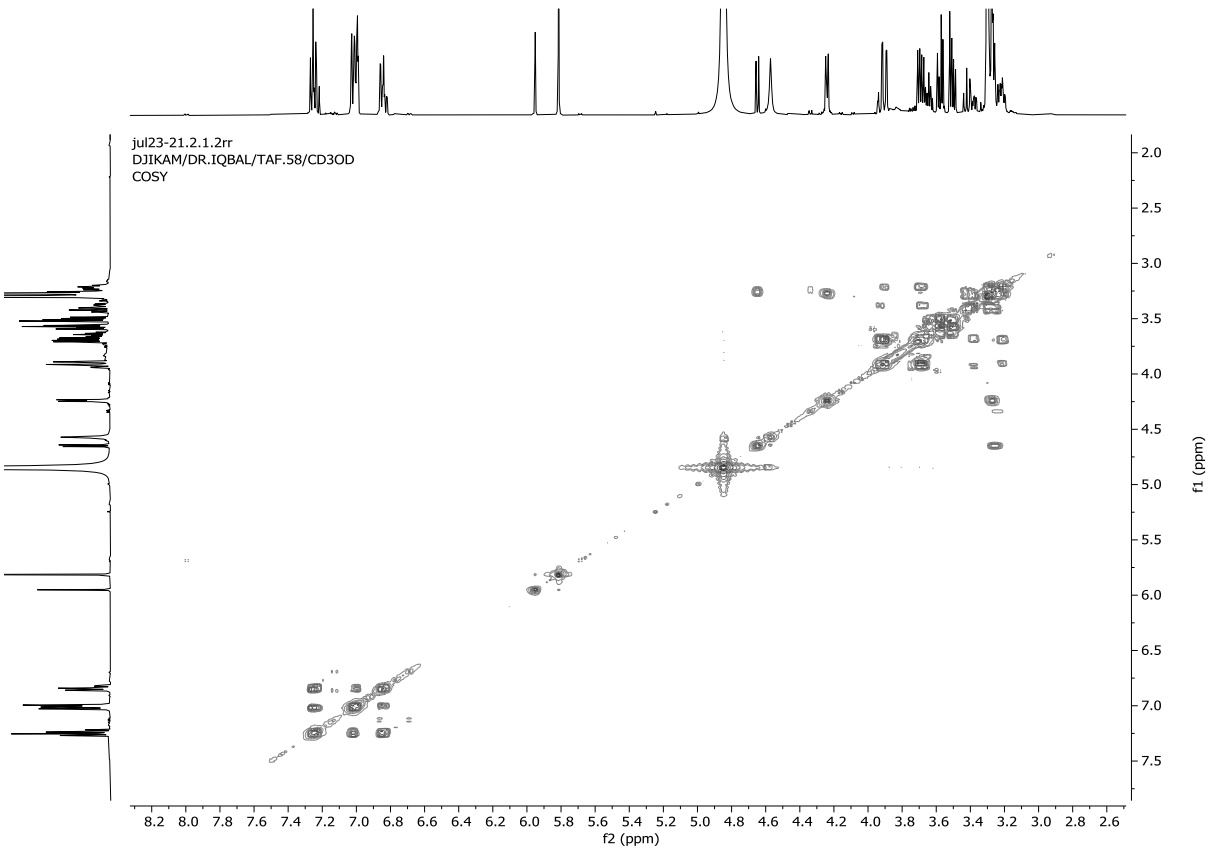

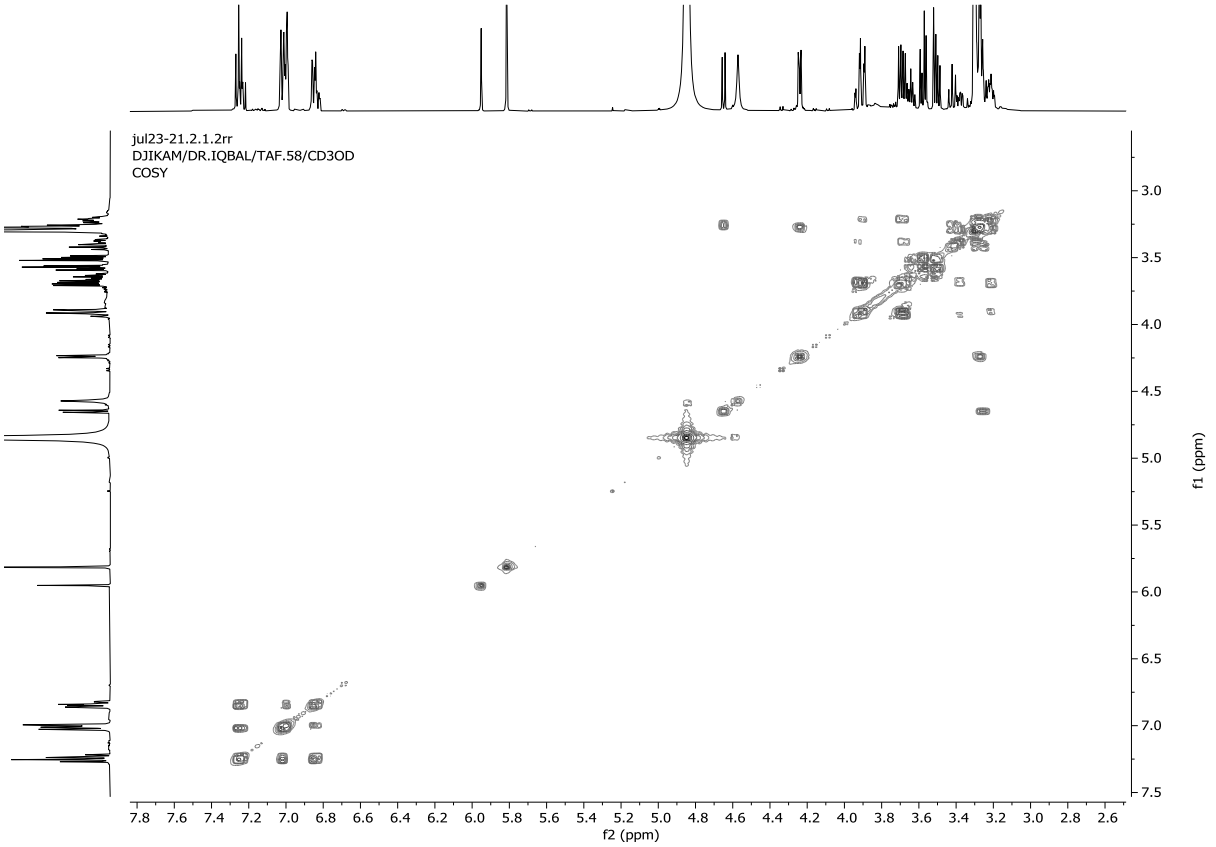

Figure S18. COSY spectrum of compound **2.**

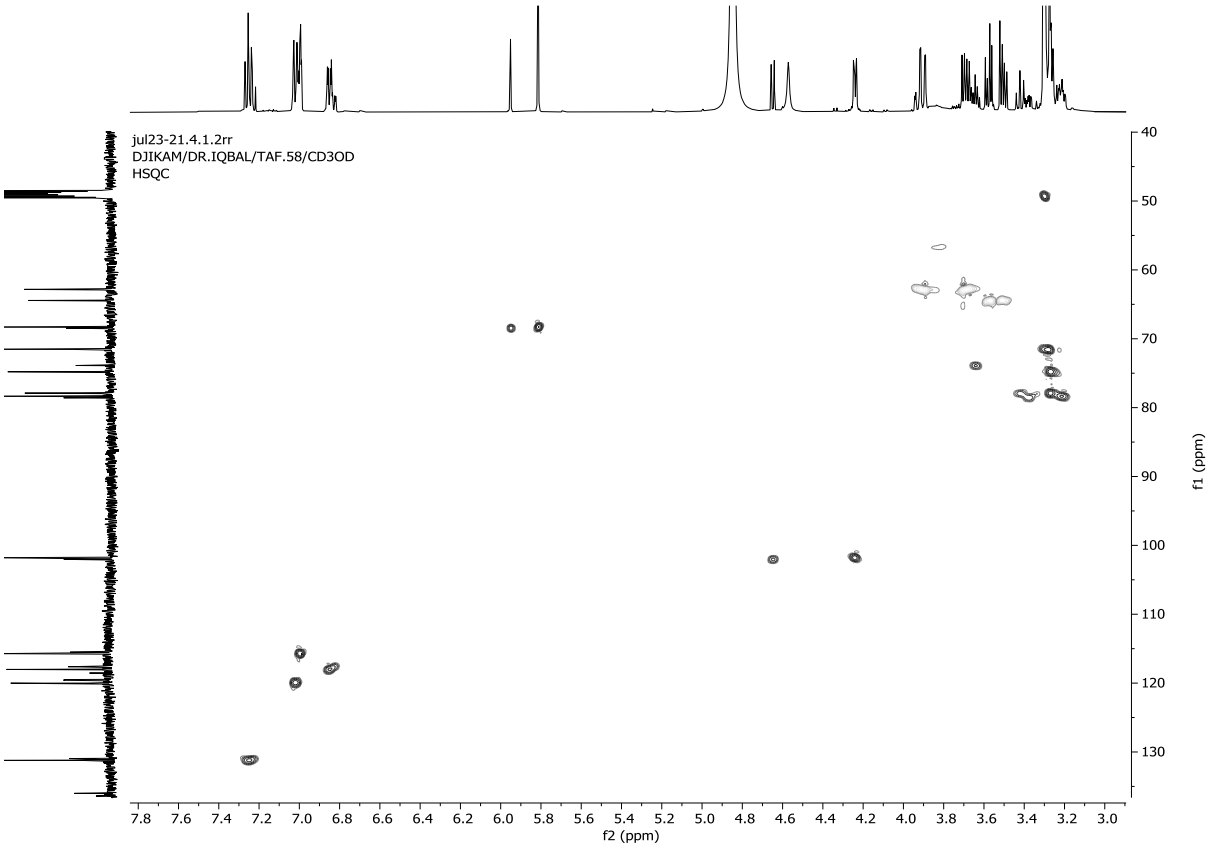

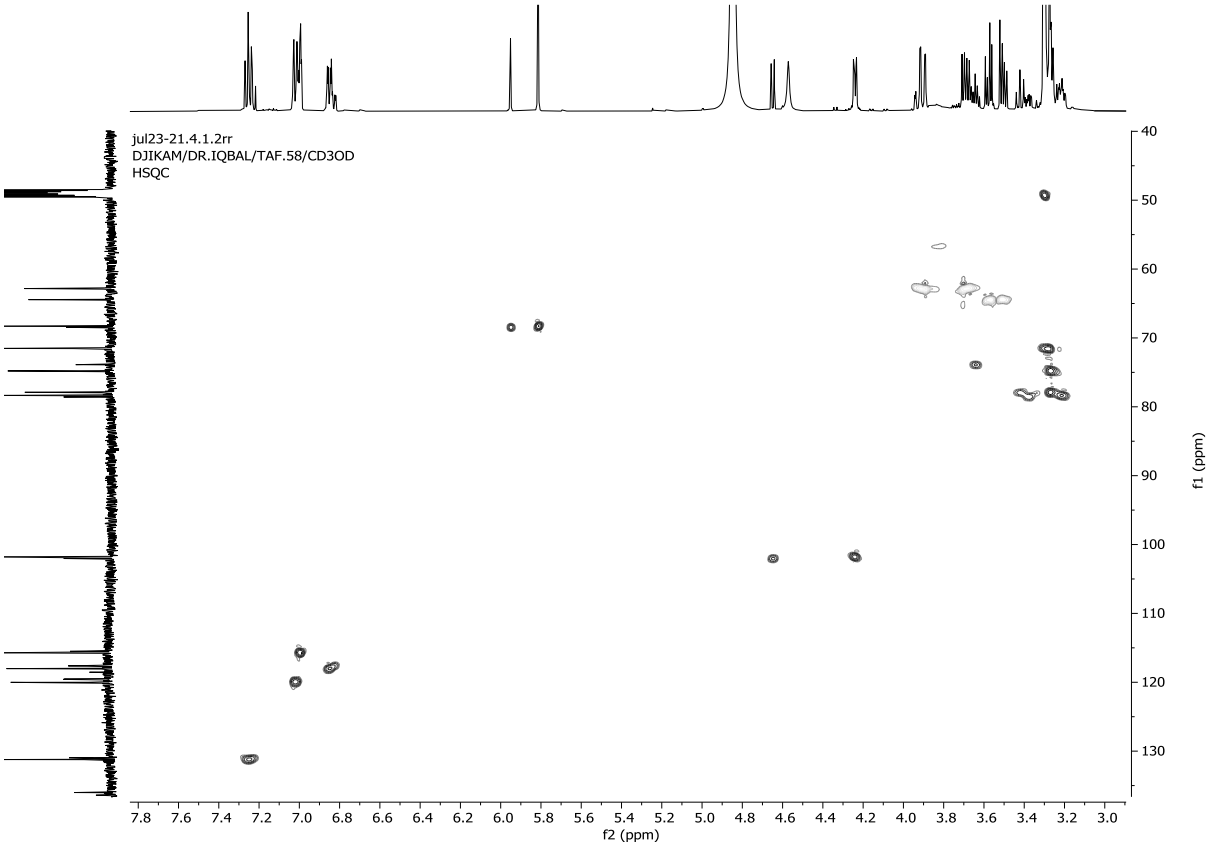

Figure S19. HSQC spectrum of compound **2.**

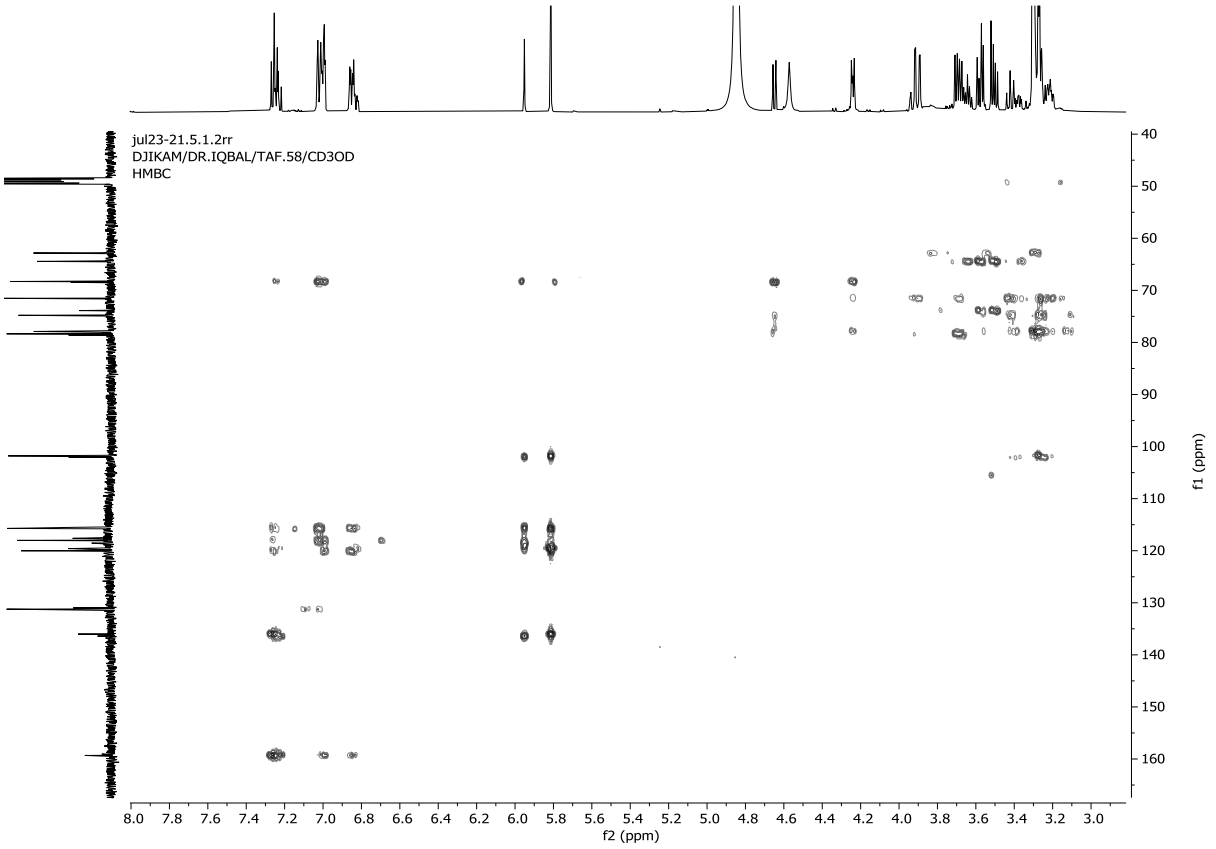

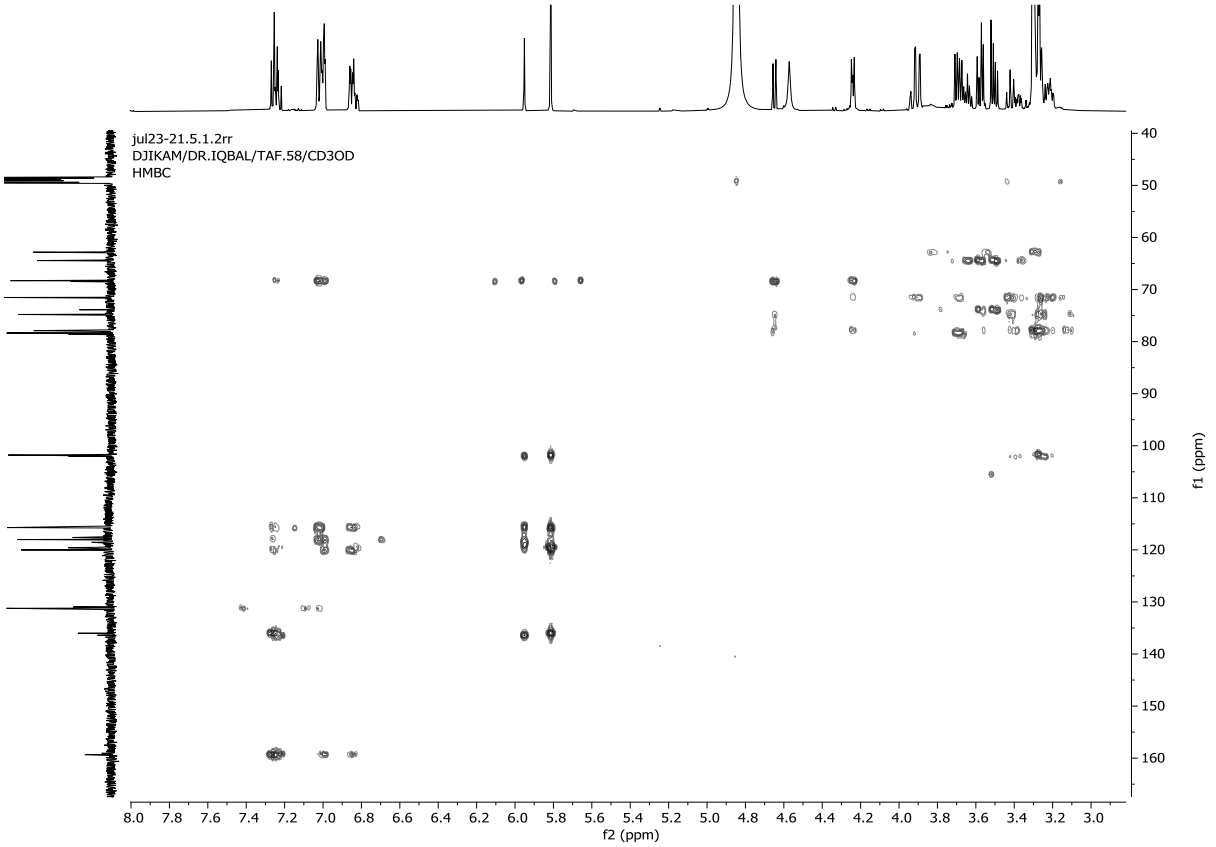

Figure S20. HMBC spectrum of compound **2.**

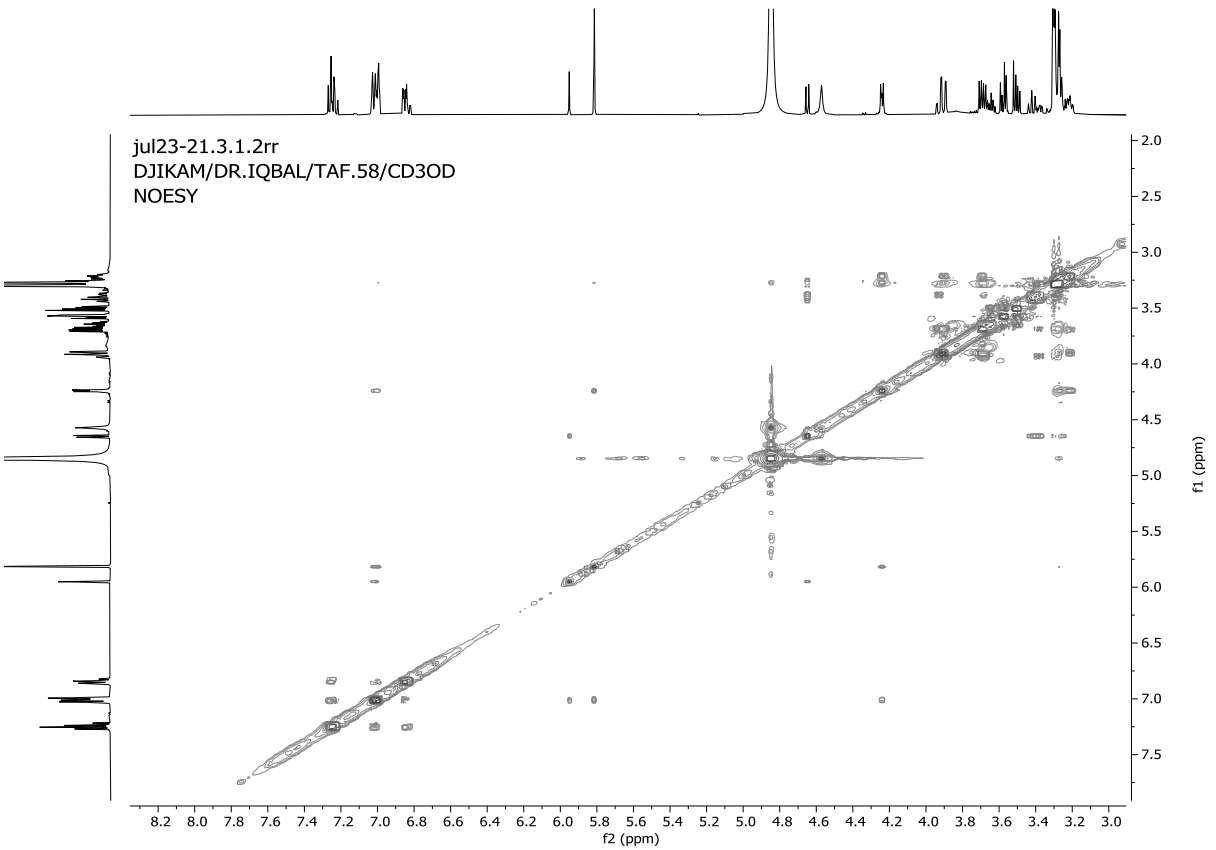

Figure S21. NOESY spectrum of compound **2.**

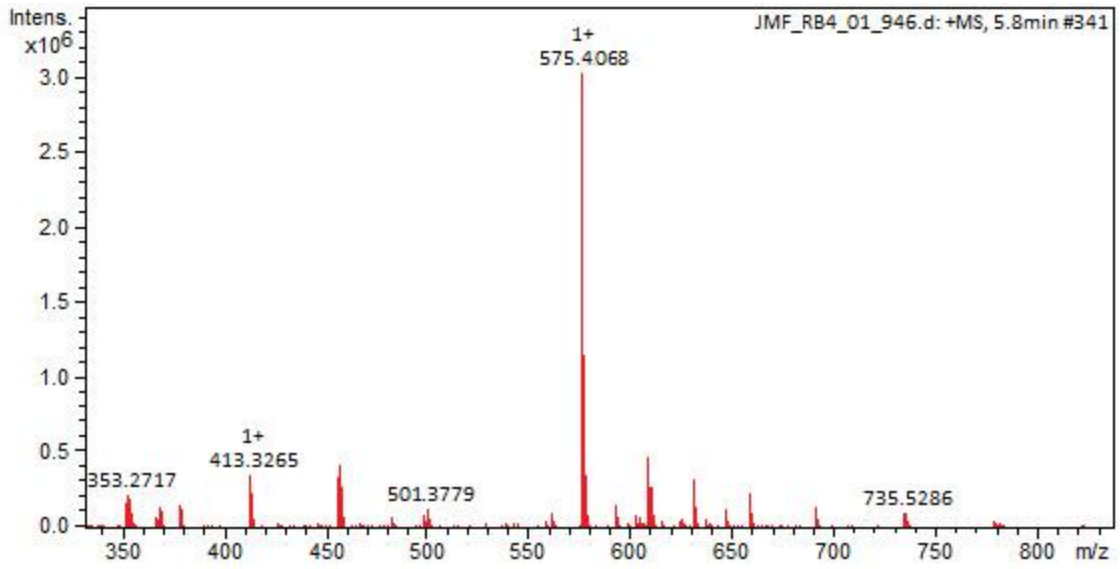

Figure S22 . LC-MS spectrum of compound **3**.

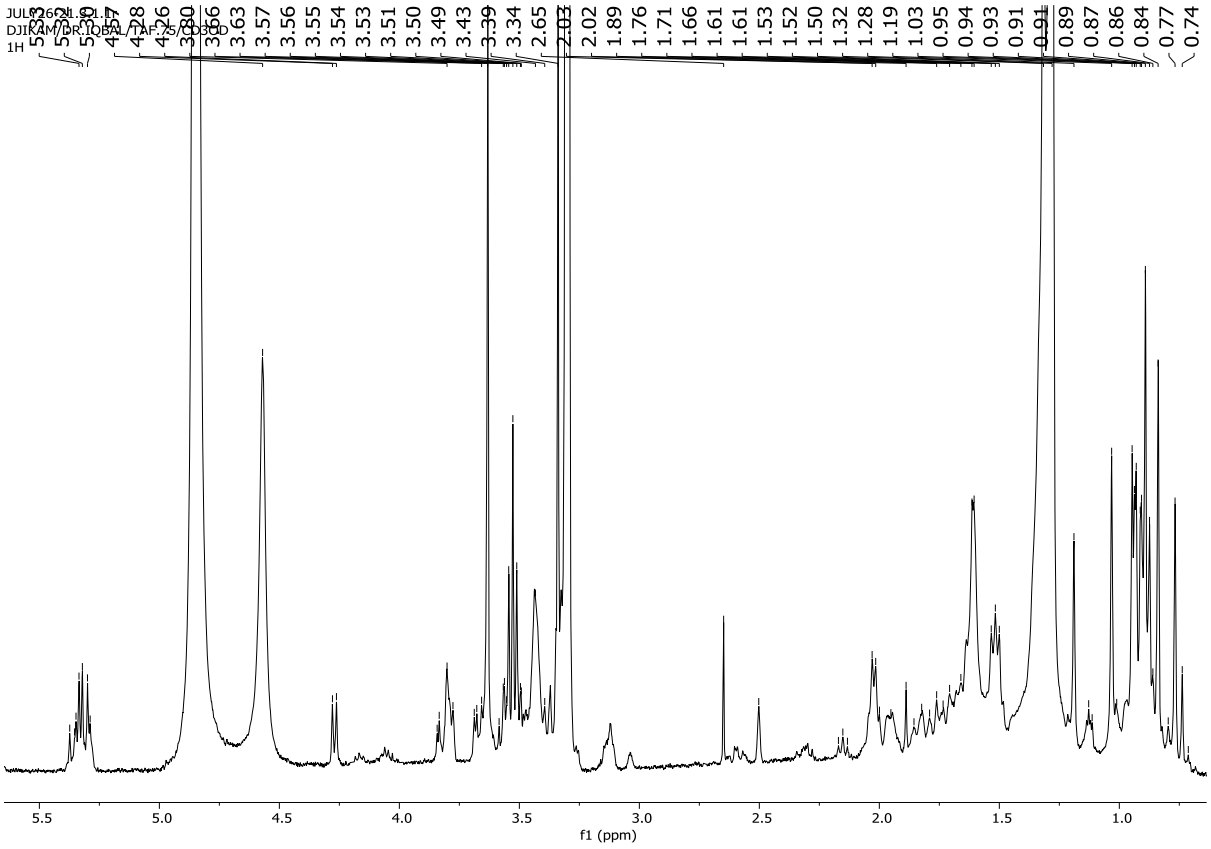

Figure S23. ^{1}H NMR spectrum of compound **3.**

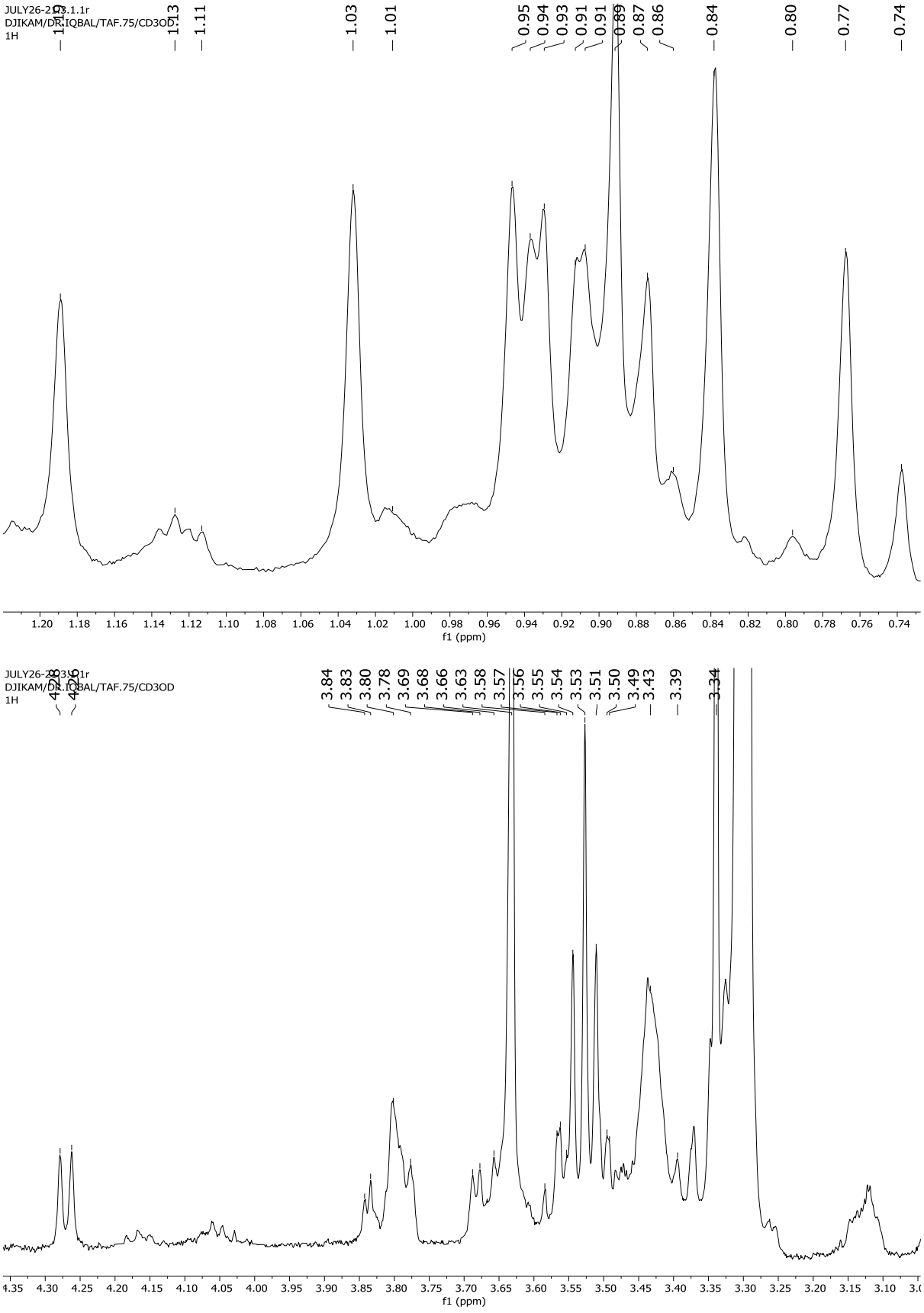

Figure S23. ^{1}H NMR spectrum of compound **3.**

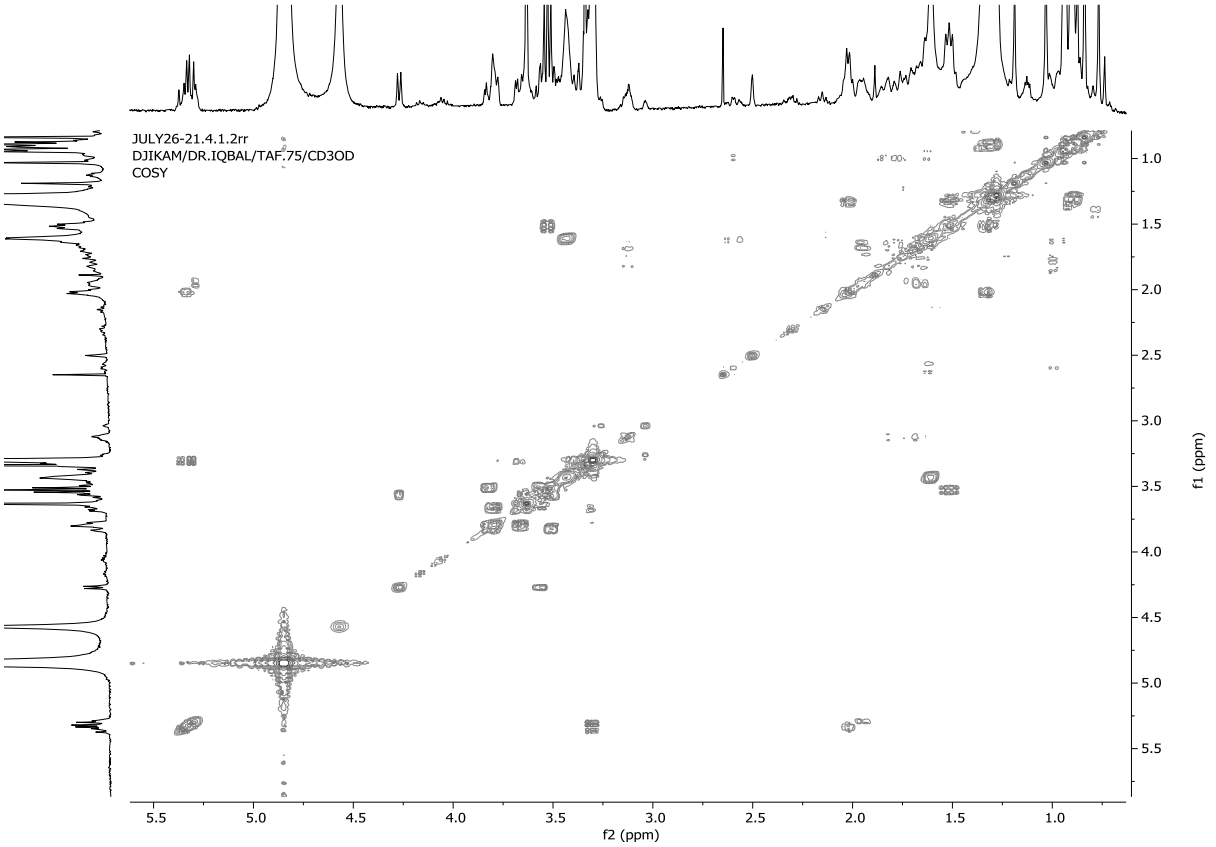

Figure S25. COSY spectrum of compound **3.**

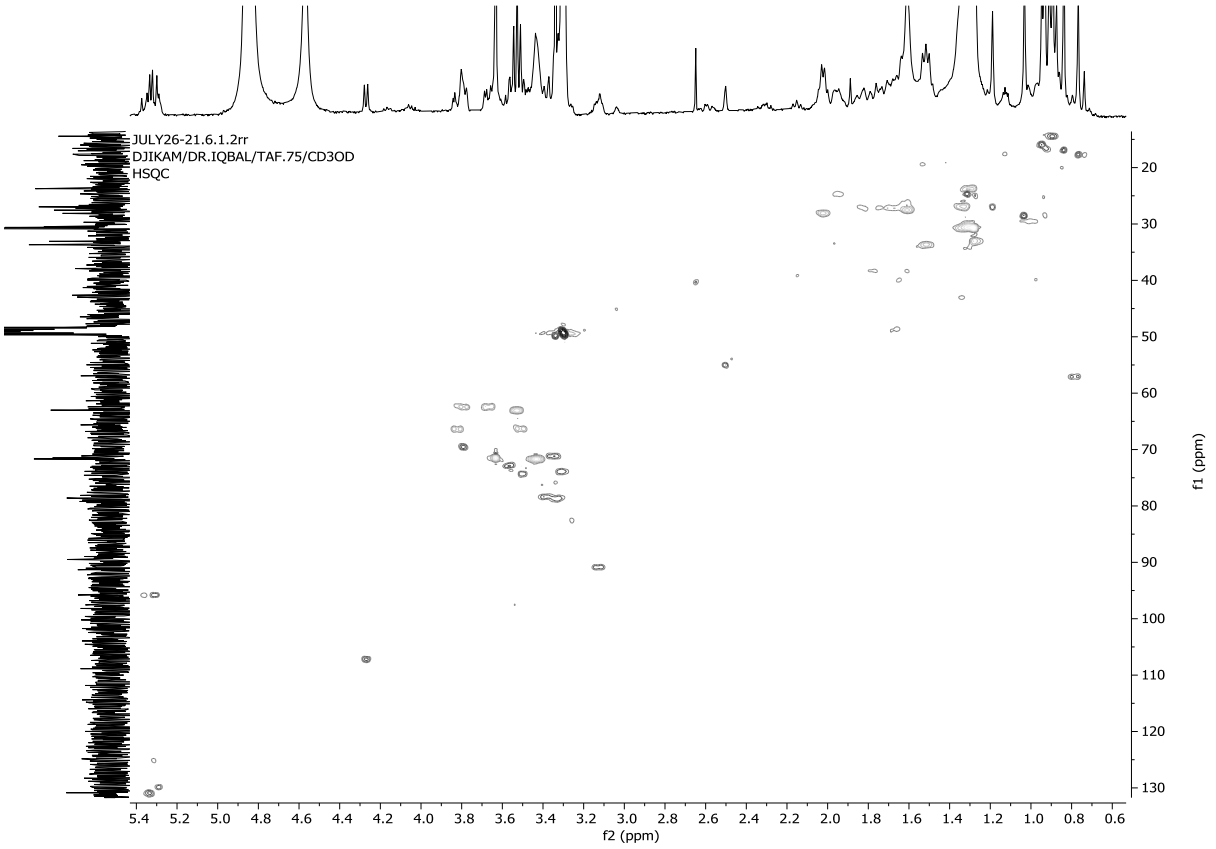

Figure S26. HSQC spectrum of compound **3.**

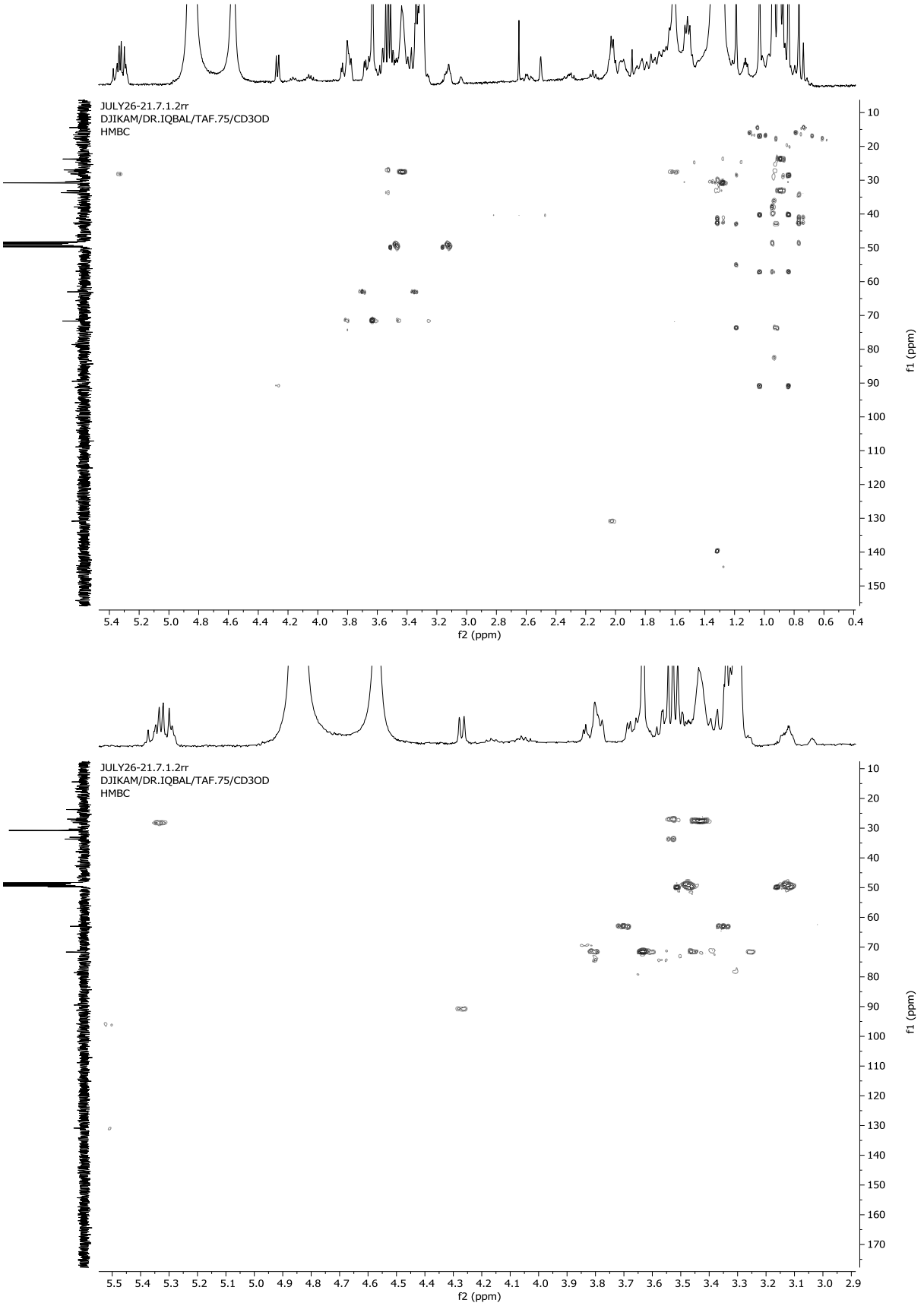

Figure S27. HMBC spectrum of compound **3.**

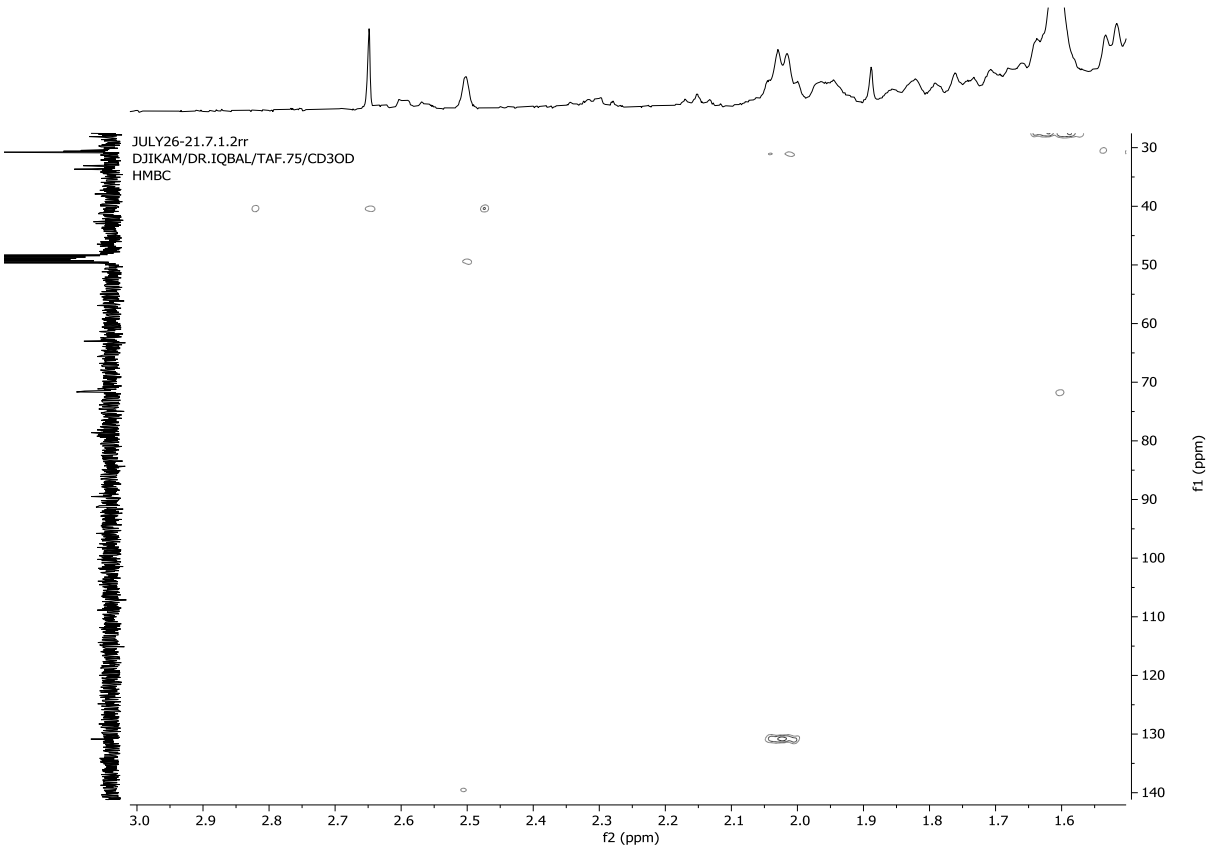

Figure S28. Expanded HMBC spectrum of compound **3.**

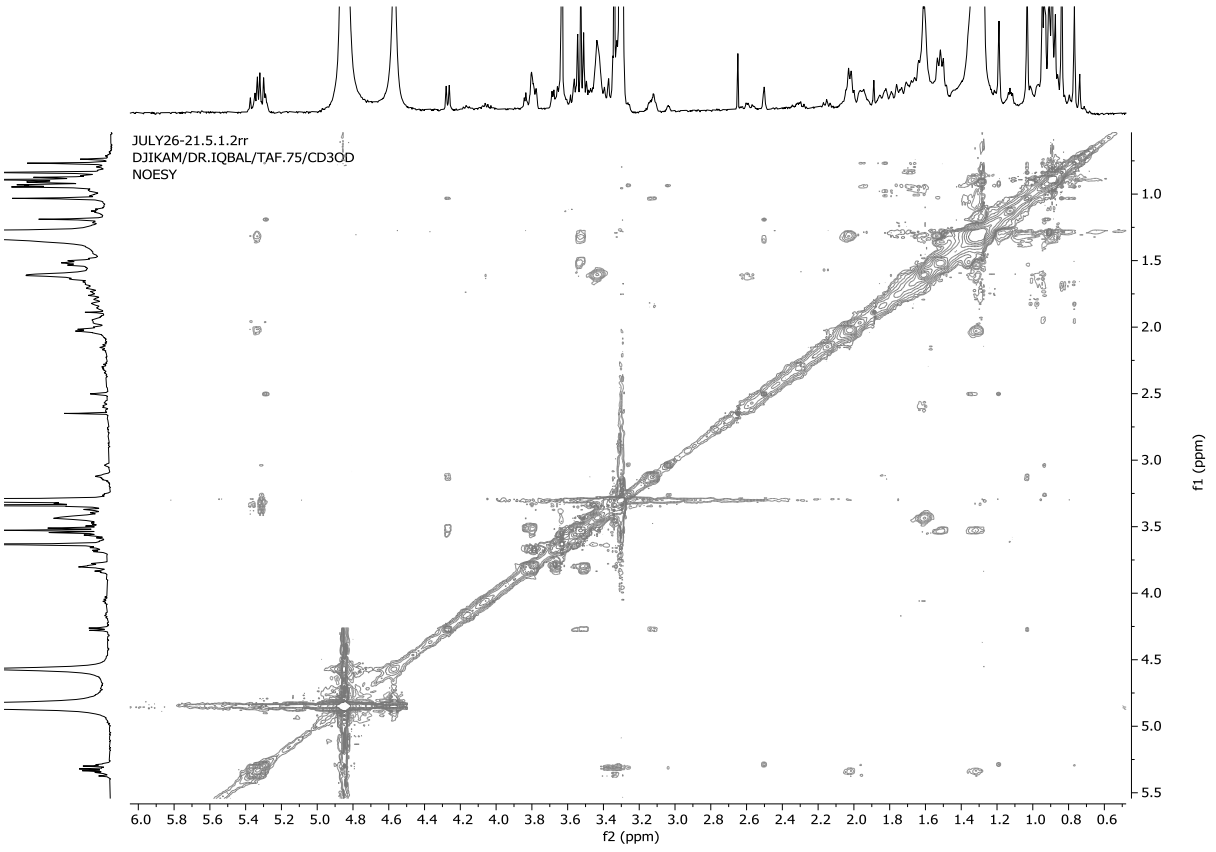

Figure S29. NOESY spectrum of compound **3.**

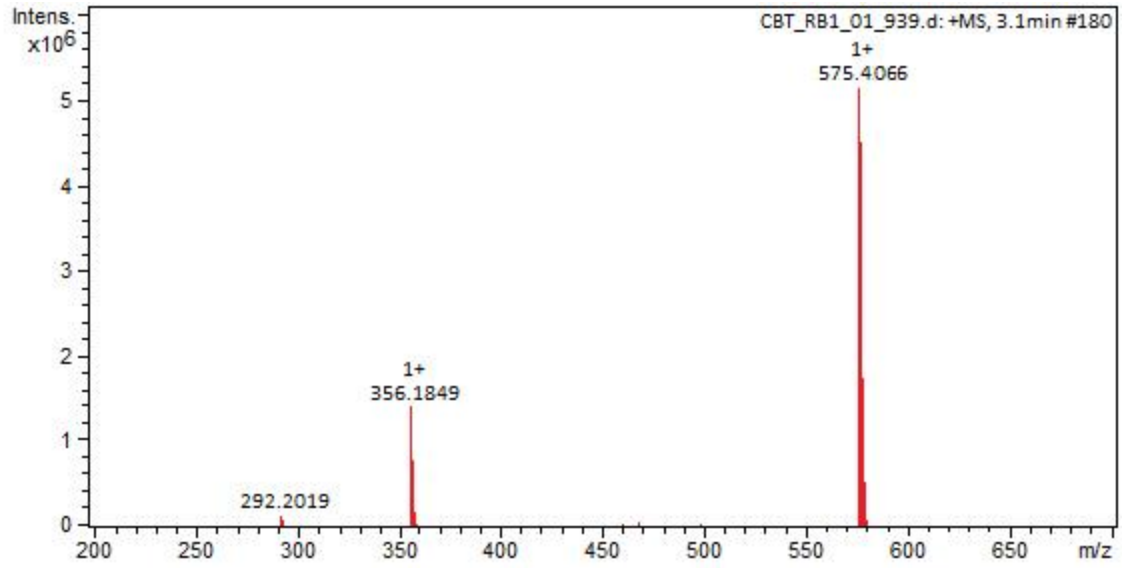

Figure S30 . LC-MS spectrum of compound **4**.

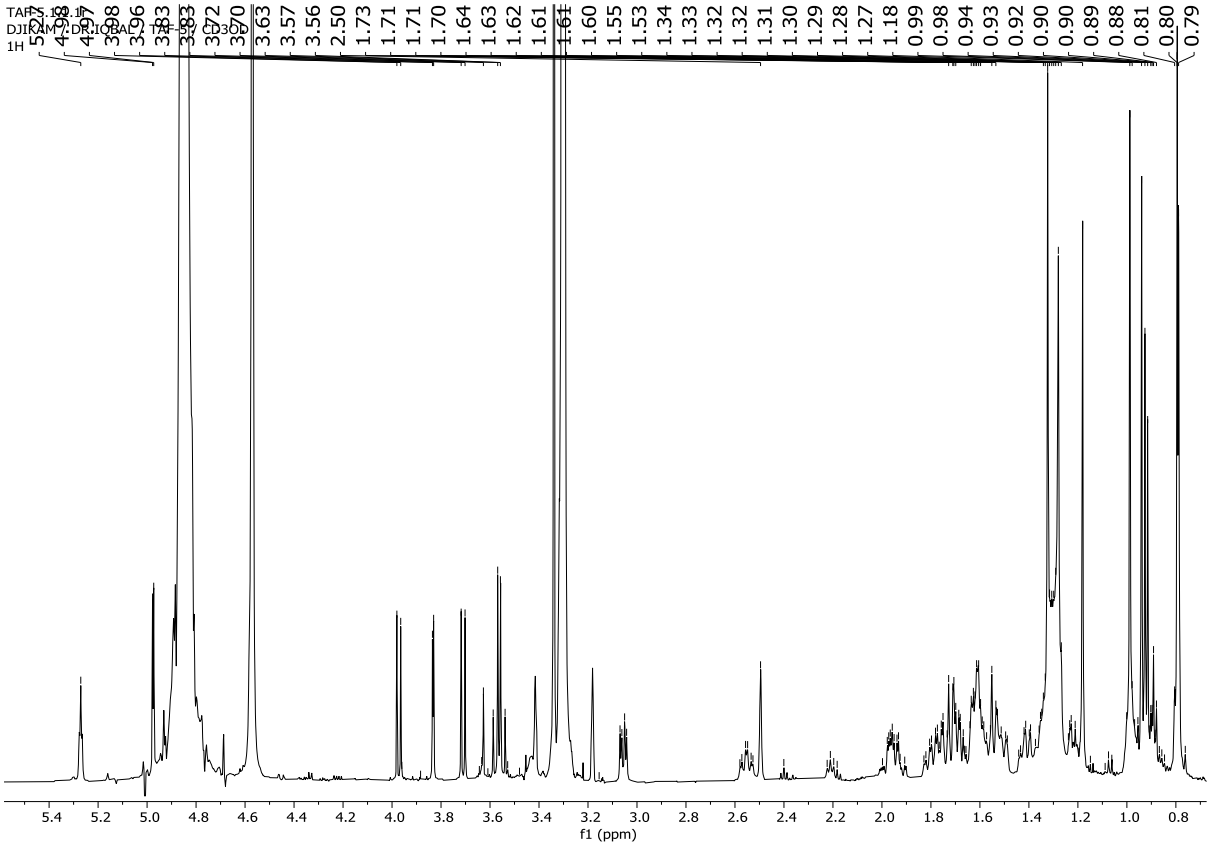

Figure S31. ^{1}H NMR spectrum of compound **4.**

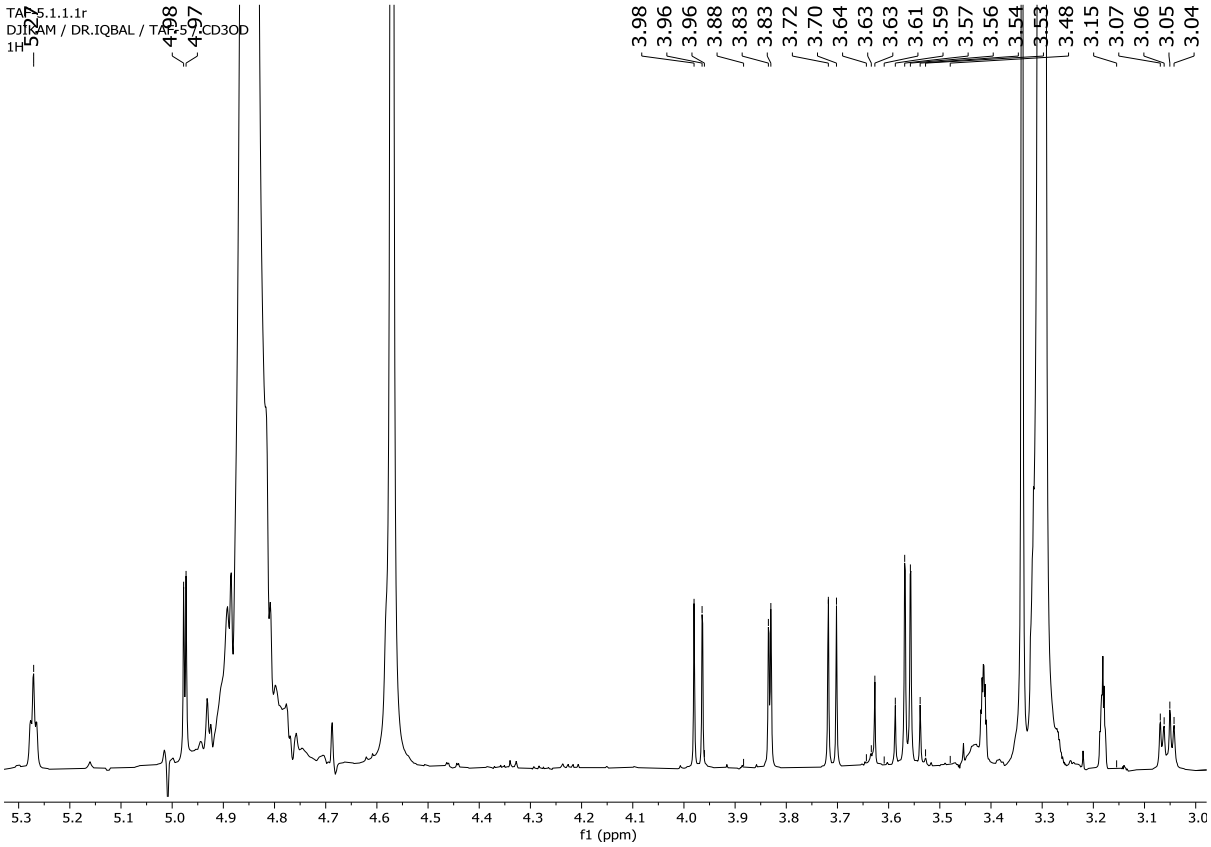

Figure S32.Expanded ^{1}H NMR spectrum of compound **4 (Apiofuranosyl moiety).**

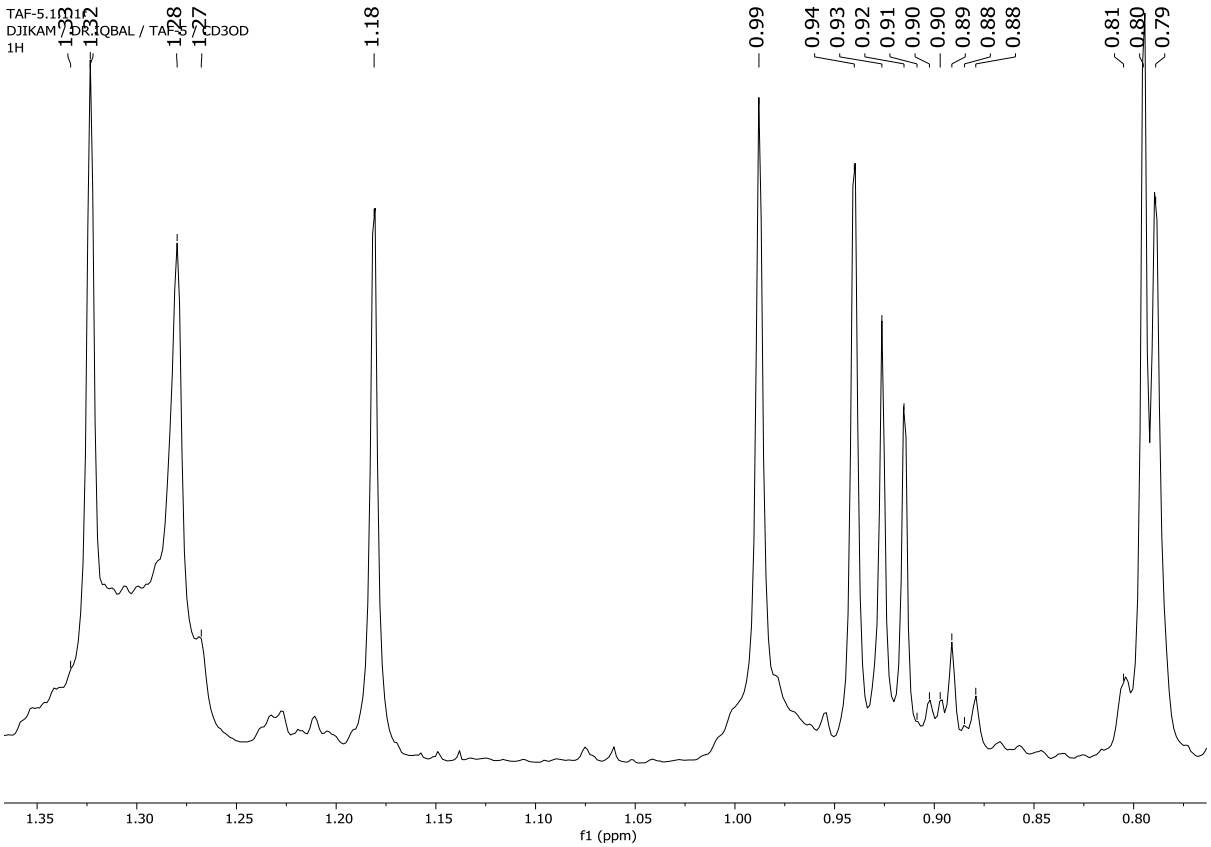

Figure S33.Expanded ^{1}H NMR spectrum of compound **4 (methyl protons).**

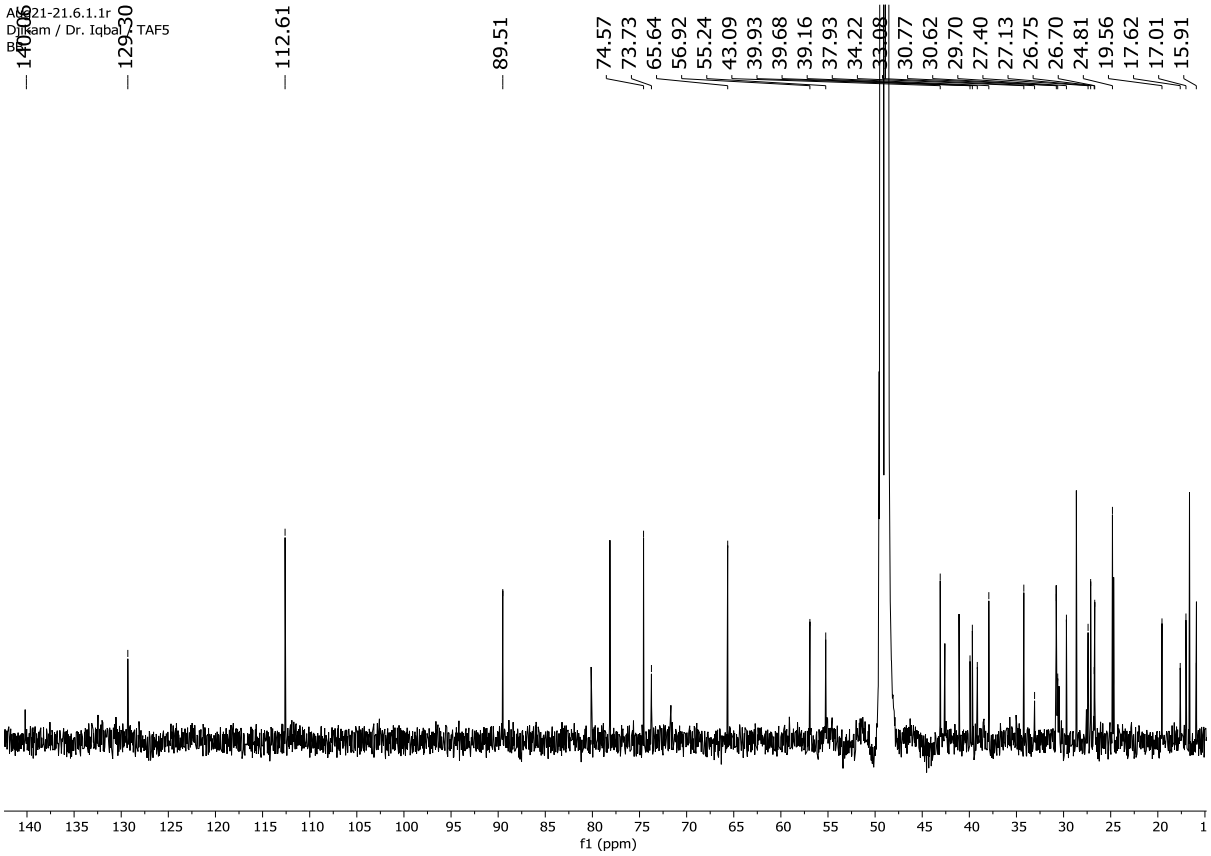

Figure S34. ^{13}C NMR spectrum of compound **4.**

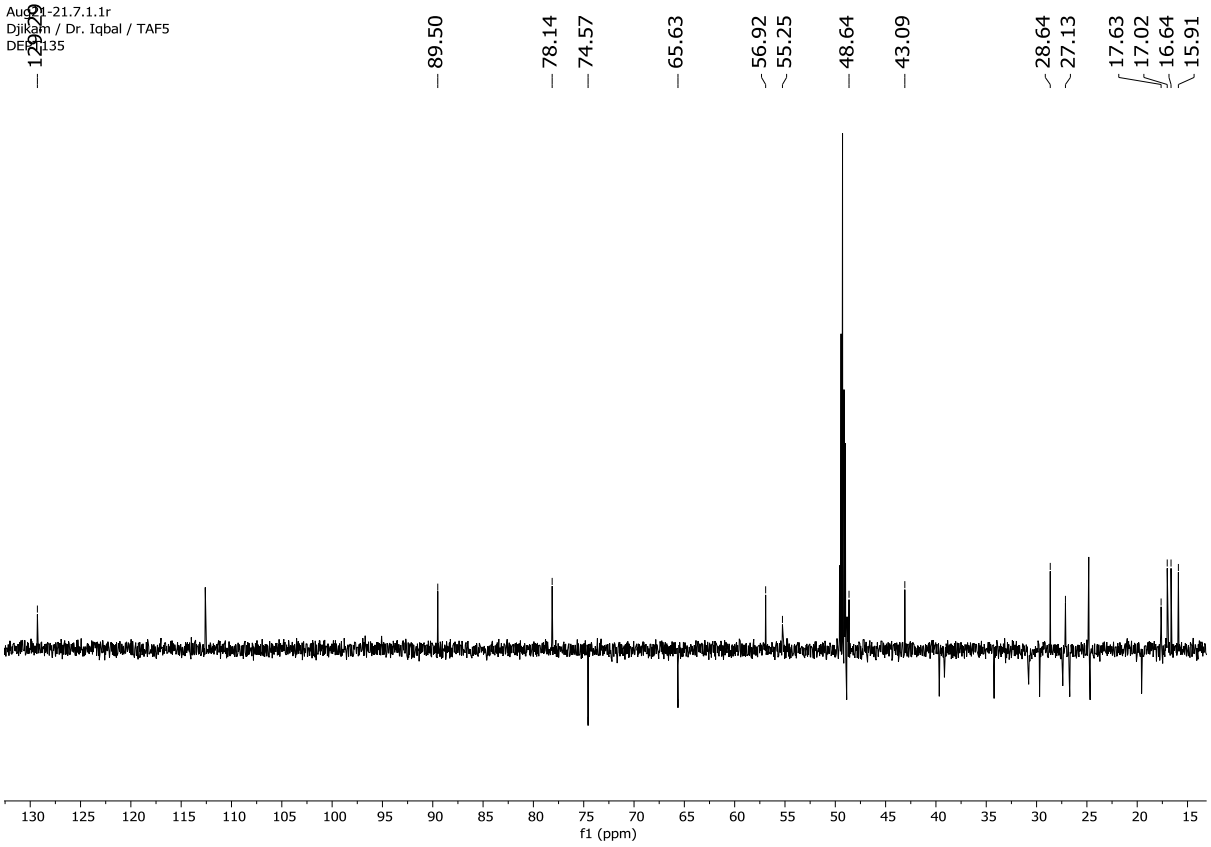

Figure S35. DEPT 135 spectrum of compound **4.**

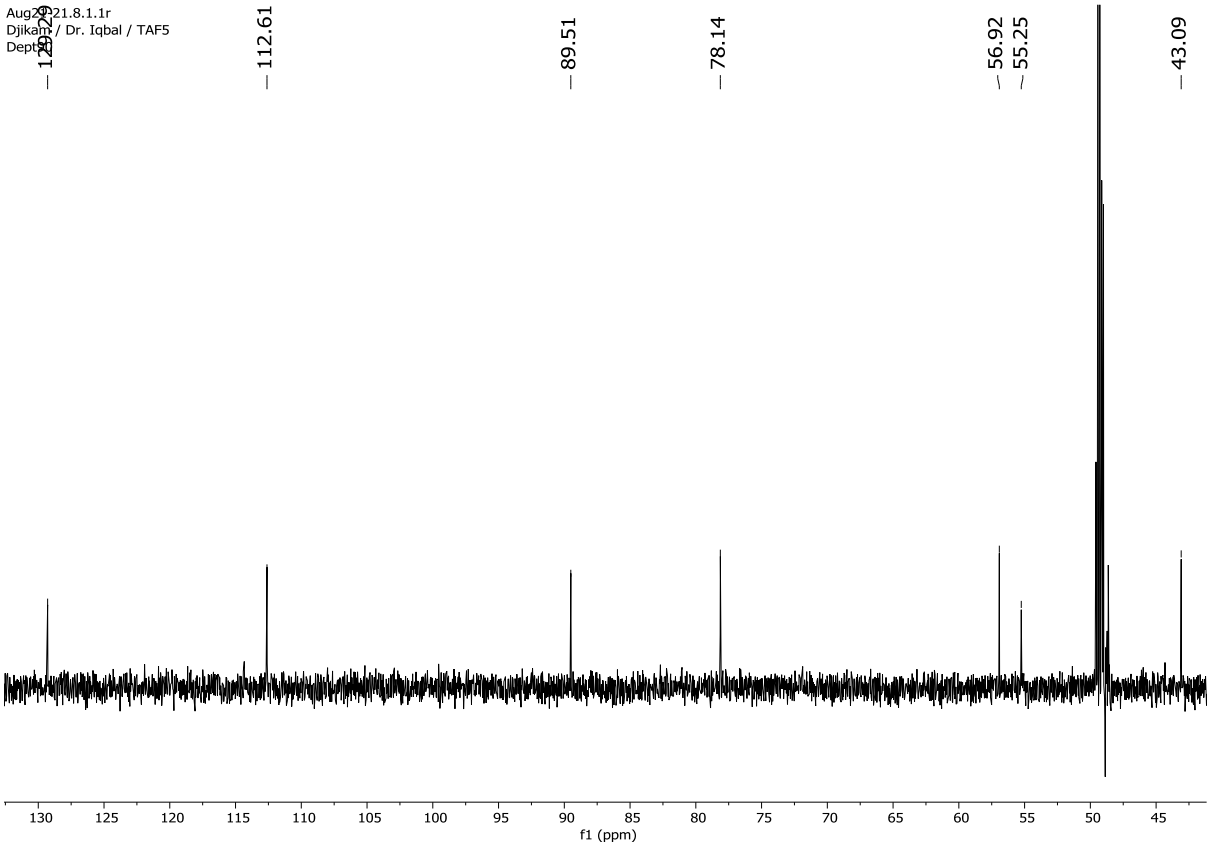

Figure S36. DEPT 90 spectrum of compound **4.**

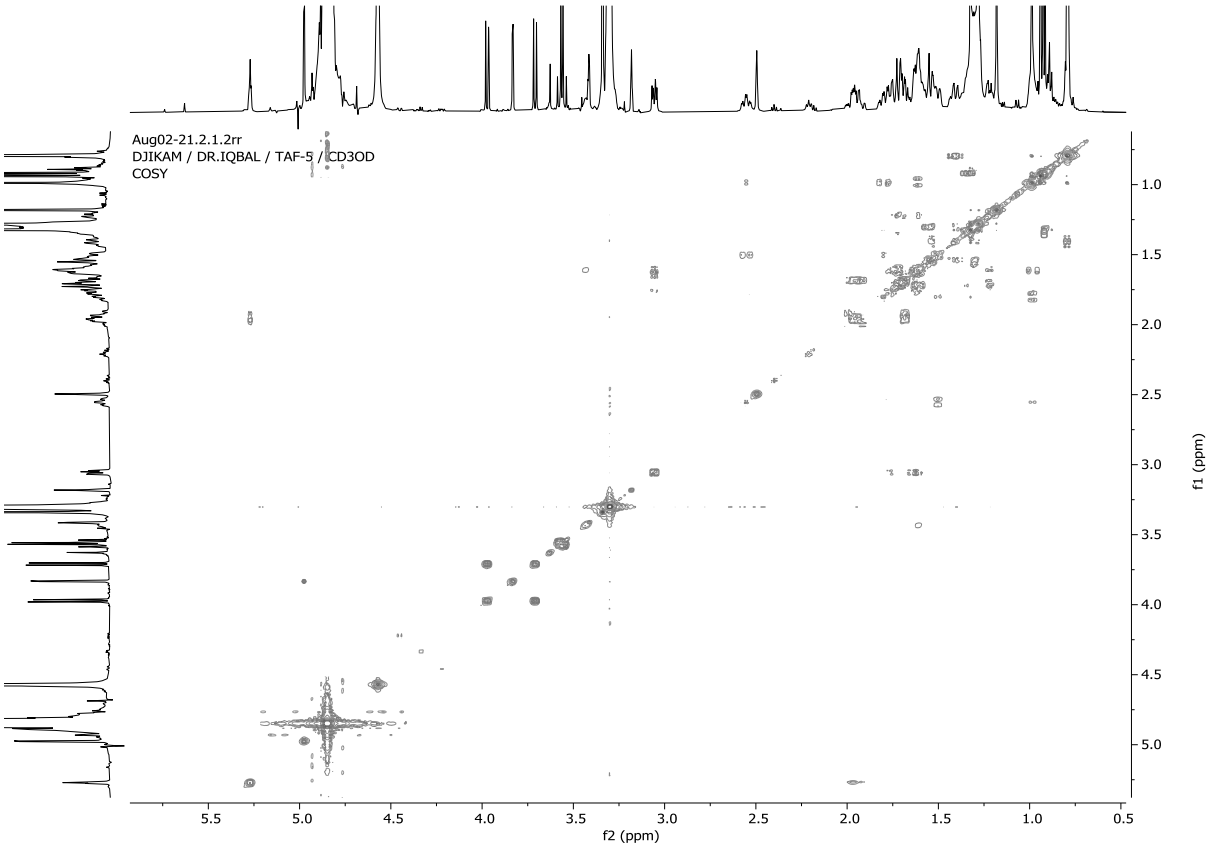

Figure S37. COSY spectrum of compound **4.**

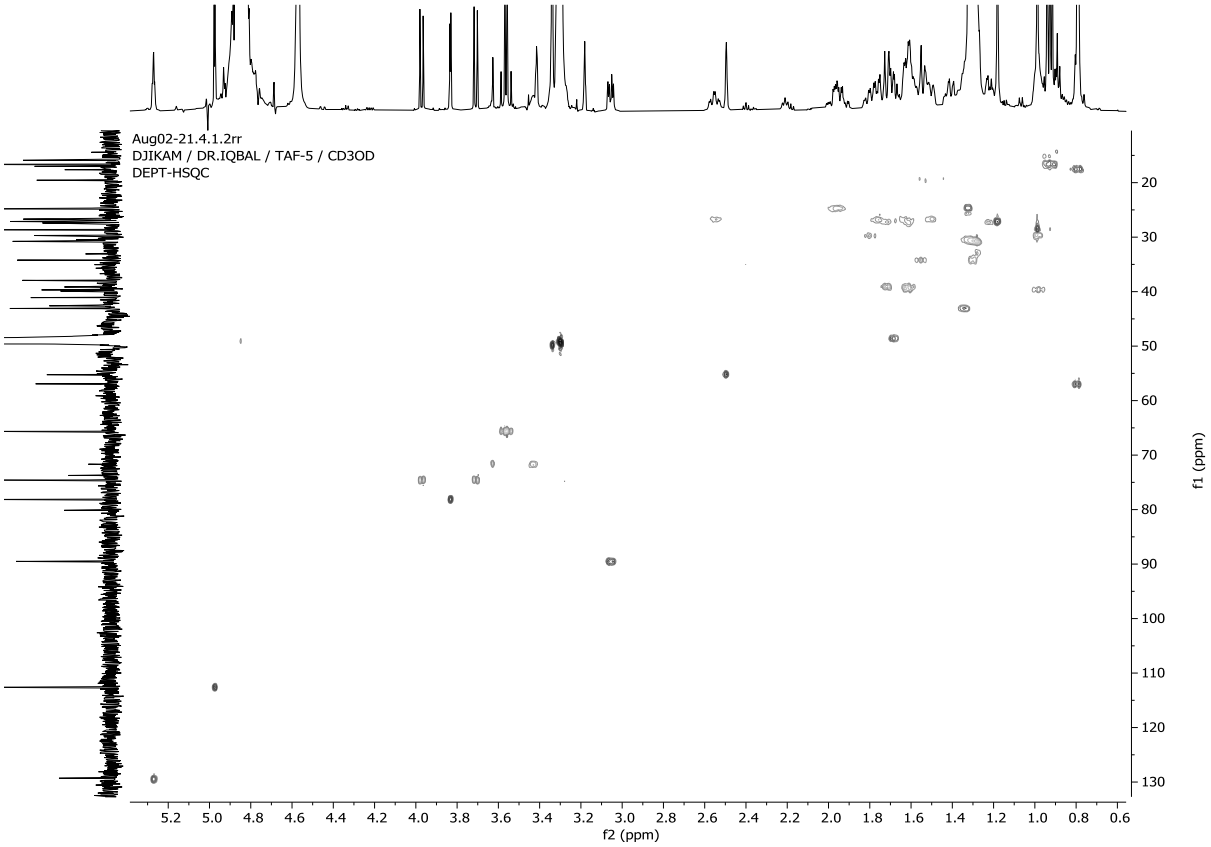

Figure S38. HSQC spectrum of compound **4.**

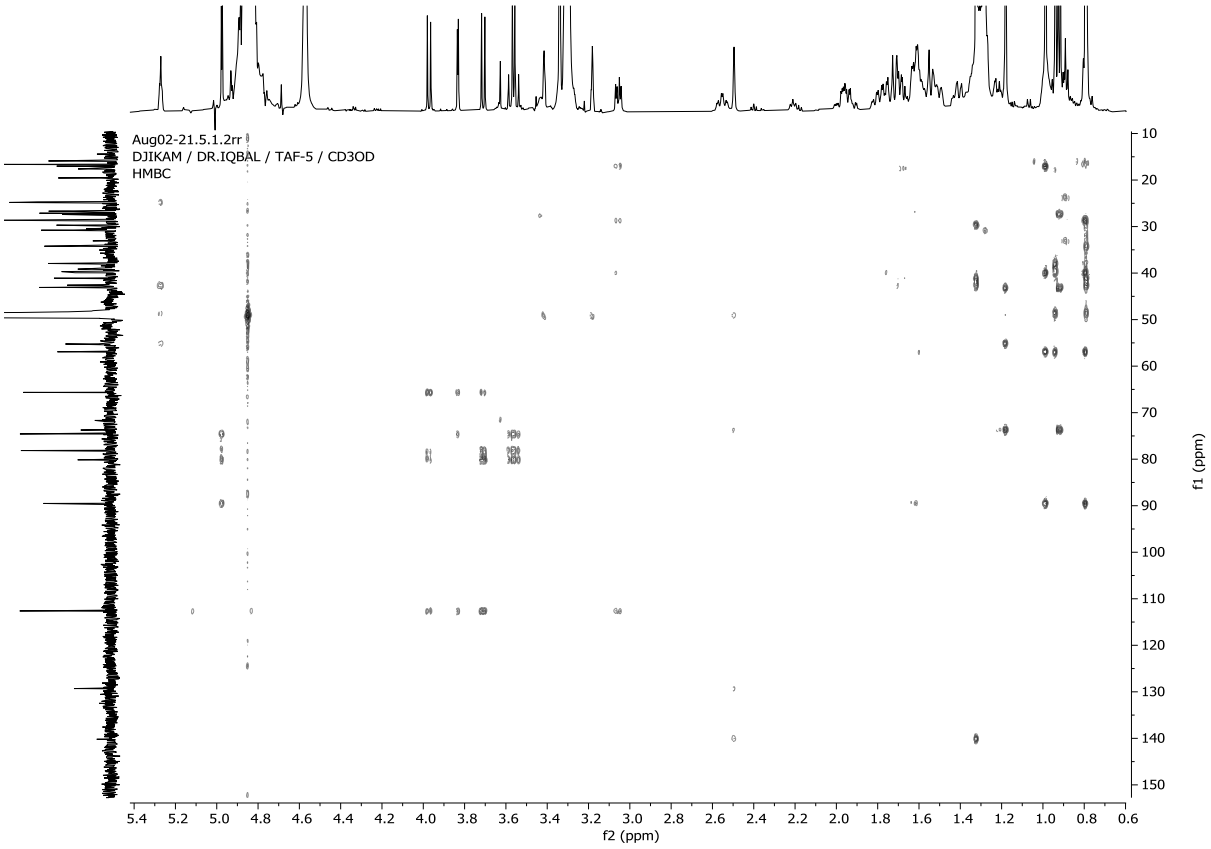

Figure S39. HMBC spectrum of compounds **4.**

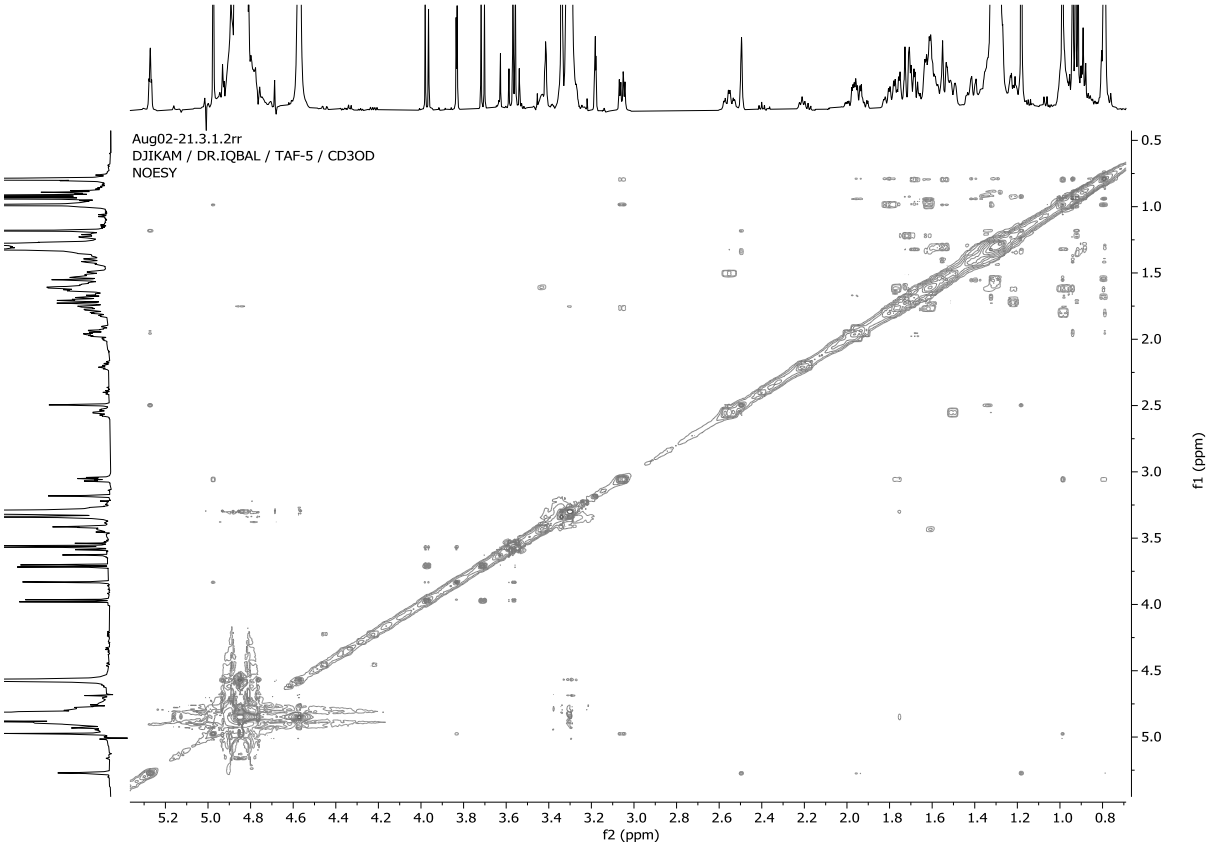

Figure S40. NOESY spectrum of compound **4.**

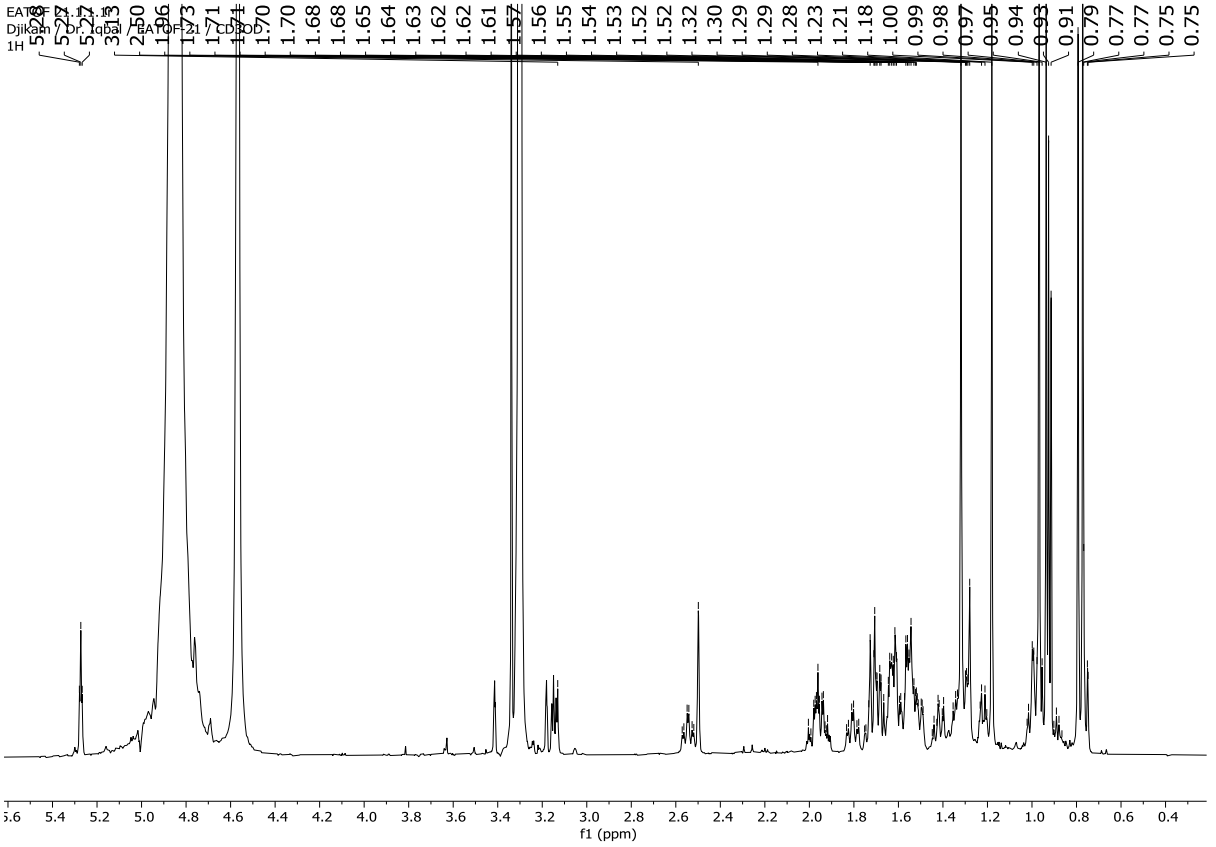

Figure S41. ^{1}H NMR spectrum of compound **5.**

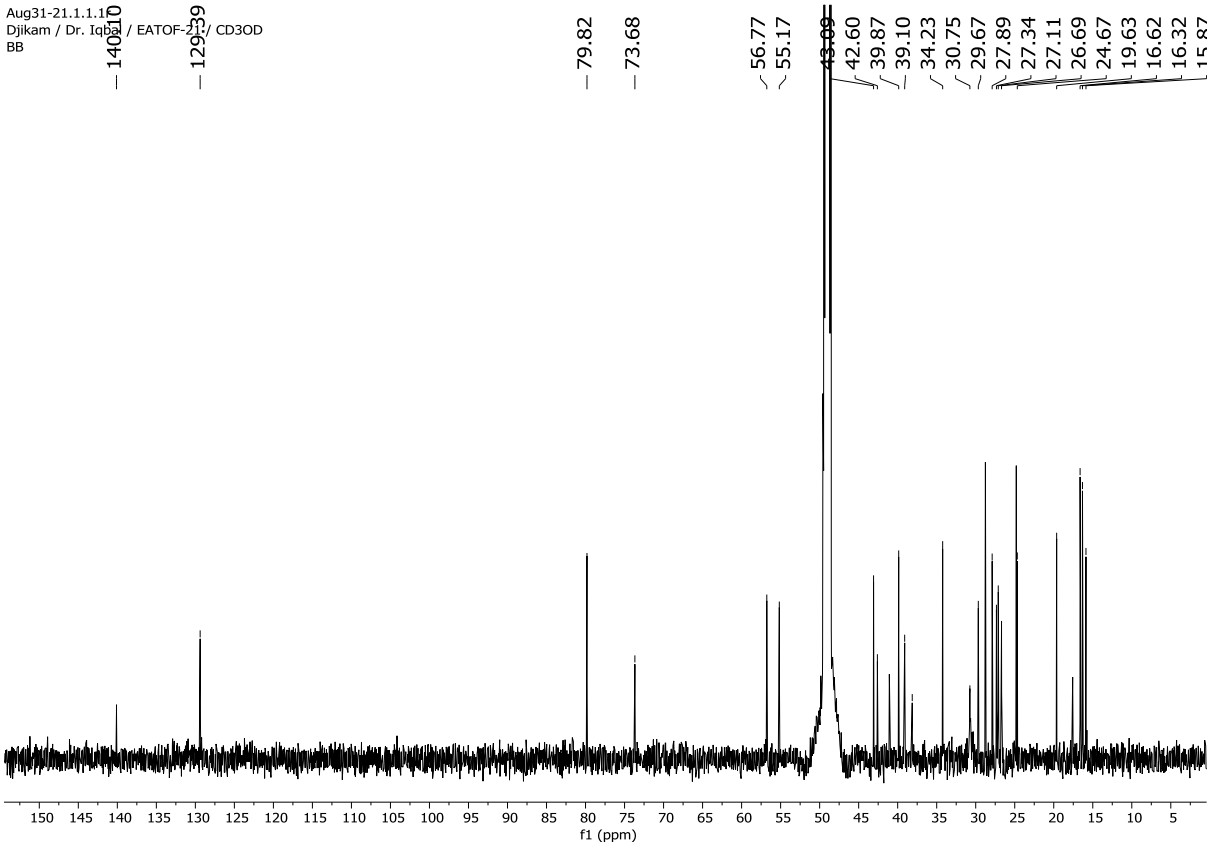

Figure S42. ^{13}C NMR spectrum of compound **5.**

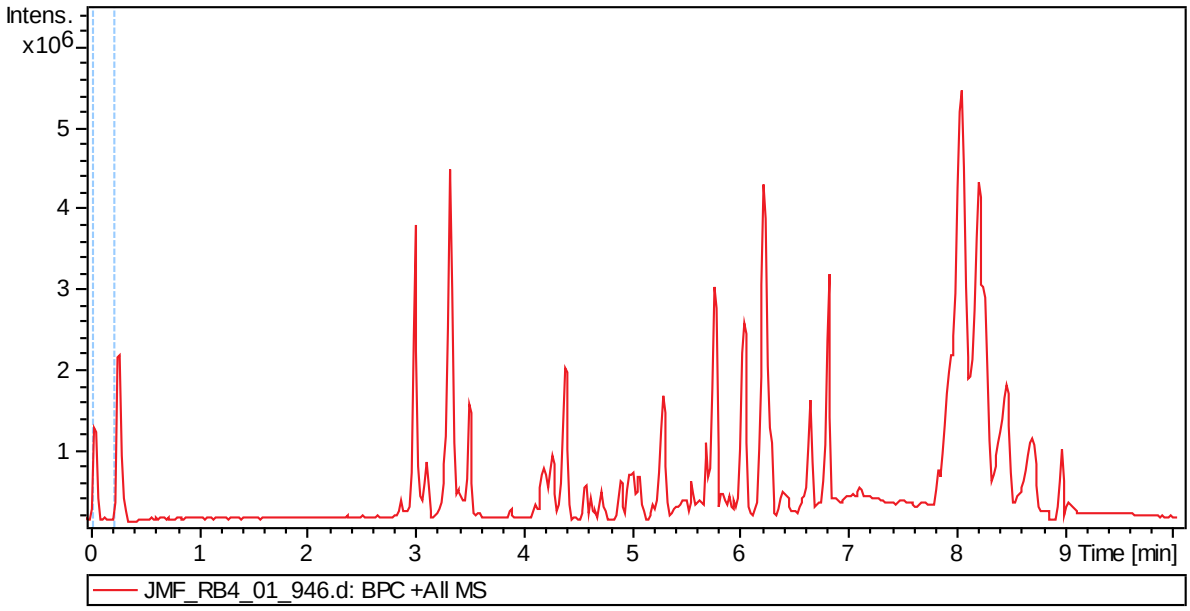

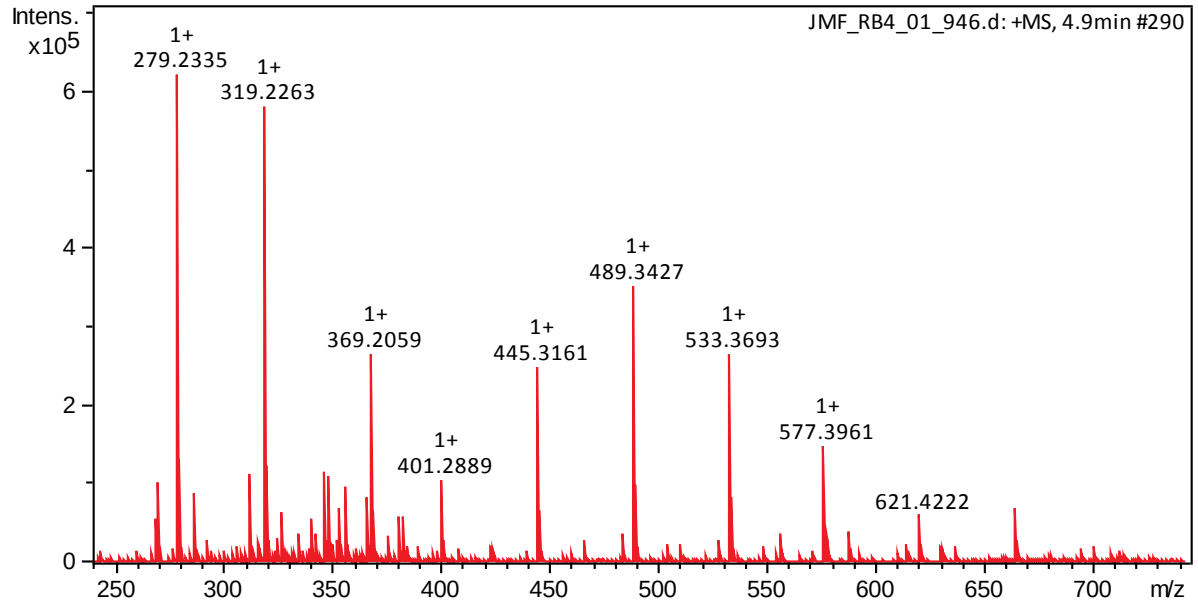

Figure S43. HPLC profile of MeOH extract of *T. atherura*.

Summary of *in vitro* antiplasmodial activity of 05 extracts

IC_{50} on *P. falciparum* 3D7 (µg/mL)

Extract's code	IC50 1	IC50 2	Mean IC50	SD
EATOF172	> 100	> 100	> 100	ND
EATOF21	> 100	> 100	> 100	ND
TAF5	> 100	> 100	> 100	ND
EATOF99	> 100	> 100	> 100	ND
EXTOFFr	7,923	7,173	7,548	0,5303301
Artemisinin (µM)	0,03746	0,03064	0,03405	0,0048225
Chloroquine (µM)	0,02947	0,02894	0,029205	0,0003748

IC_{50} on *P. falciparum* Dd2 (µg/mL)

Extract's code	IC50 1	IC50 2	Mean IC50	SD
EATOF172	55,34	74,65	64,995	13,654232
EATOF21	73,51	76,25	74,88	1,9374726
TAF5	94,97	89,62	92,295	3,7830213
EATOF99	72,3	73,74	73,02	1,0182338
EXTOFFr	4,196	4,59	4,393	0,2786001
Artemisinin (µM)	0,05134	0,03533	0,043335	0,0113208
Chloroquine (µM)	0,5816	0,6998	0,6407	0,08358

Figure S45. Antiplasmodial test of extract and pure compounds**.**

References

Trager W, Jensen JB. 1976. Human malaria parasites in continuous culture. *Science* 193: 673–675.

Kaushik NK, Bagavan A, Rahuman AA, Zahir AA, Kamaraj C, Elango G, Jayaseelan C, Kirthi AV, Santhoshkumar T, Marimuthu S, Rajakumar G, Tiwari SK, sahal D. 2015. Evaluation of antiplasmodial activity of medicinal plants from North Indian Buchpora and South Indian Eastern Ghats, Malar J. 14 (2015) 65. Doi: 10.1186/s12936-015-0564-z.

Smilkstein M, Sriwilaijaroen N, Kelly JX, Wilairat P, Riscoe M. 2004. Simple and inexpensive fluorescence-based technique for high-throughput antimalarial drug screening, Antimicrob Agents Chemother. 48: 1803–1806.

Lambros C, Vanderberg JP. 1979. Synchronization of *Plasmodium falciparum* erythrocytic stages in culture, J. Parasitol. 65: 418–420.

Mosmann T. 1983. Rapid colorimetric assay for cellular growth and survival: application to proliferation and cytotoxicity assays. J Immunol Methods 65: 55–63.